

REPORT



## Maximizing activity and selectivity of antibody-mediated effector functions using antibody mixtures

Tiexin Wang<sup>a,b</sup>, Alec A. Desai<sup>b</sup>, Greg M. Thurber<sup>a,c</sup>, and Peter M. Tessier<sup>a,b,c,d</sup>

<sup>a</sup>Department of Chemical Engineering, University of Michigan, Ann Arbor, MI, USA; <sup>b</sup>Biointerfaces Institute, University of Michigan, Ann Arbor, MI, USA; <sup>c</sup>Department of Biomedical Engineering, University of Michigan, Ann Arbor, MI, USA; <sup>d</sup>Department of Pharmaceutical Sciences, University of Michigan, Ann Arbor, MI, USA

### ABSTRACT

Fc-mediated effector functions are key for conferring potent antibody-mediated killing of cancer cells. However, it is difficult to achieve highly selective targeting of cancer cells while minimizing toxicity on healthy tissue because of the expression of most receptors, albeit at lower levels, on non-cancer cells. Previous attempts to increase the selectivity of antibody-mediated effector functions have sought to reduce binding affinity and/or increase avidity, which typically results in modest improvements in selectivity. To overcome this limitation, we report the use of mixtures of antibody variants that achieve high selectivity based on receptor level while maintaining high activity for cells with high receptor levels. We have studied mixtures of two variants of an anti-HER2 antibody (trastuzumab), one that is affinity-reduced and effector-competent and a second high-affinity variant that is effectorless. Notably, we observe that the high-affinity, effectorless antibody reduces effector function for cells with low receptor levels, including reduced antibody-dependent cellular cytotoxicity (ADCC) and phagocytosis (ADCP), while the high-avidity, effector-competent antibody mediates significant effector function for cells with high receptor levels. Moreover, replacing the effector-competent Fc region of the affinity-reduced antibody with high-affinity Fc domains that enhance effector function drives high activity while maintaining high selectivity for the antibody mixtures. These findings outline a general strategy for maximizing the therapeutic window by selectively targeting cancer cells based on receptor levels that could be applied to a wide range of applications involving antibody-mediated synapse formation, including antibody-drug conjugates and bispecific antibodies, such as T cell engagers.

### ARTICLE HISTORY

Received 28 May 2024  
Revised 17 February 2025  
Accepted 12 March 2025

### KEYWORDS

Avidity; ADCC; ADCP; cancer; HER2; mAb; trastuzumab; toxicity; therapeutic window

### Introduction





Monoclonal antibodies (mAbs) are widely used as cancer therapeutics for targeting both cancer cells and immune receptors. A critical part of their therapeutic activity is due to their Fc-mediated effector functions, such as antibody-dependent cellular cytotoxicity (ADCC) and antibody-dependent cellular phagocytosis (ADCP).<sup>1</sup> For example, ADCC has been shown to play an important role in the cytotoxic activity of several antibody therapeutics, including antibodies against tumor-associated antigens, such as epidermal growth factor receptor (EGFR), human epidermal growth factor receptor 2 (HER2), and B-lymphocyte antigen CD20.<sup>2–5</sup> ADCC also contributes to antibodies targeting immune checkpoints, such as cytotoxic T-lymphocyte-associated protein 4 (CTLA-4), by clearing regulatory T cells.<sup>6</sup> ADCP has also been shown to play an important role in therapeutic efficacy for multiple antibodies, including those against CD20 and CD38.<sup>7,8</sup>


Given the importance of such effector activity, substantial efforts have been made to enhance antibody-mediated effector functions. One approach is to engineer the Fc region to more strongly bind to activating Fcγ receptors and more weakly to

inhibitory receptors, which has been used to enhance the effector functions of the anti-HER2 antibody margetuximab.<sup>9,10</sup>

A second approach is to improve Fc binding to Fcγ receptors via afucosylation, as employed by the antibody-drug conjugate (ADC) belantamab mafodotin.<sup>11</sup> A third approach is not to rely on the Fc region for mediating the primary effector function, but rather use bispecific antibodies to recruit T cells to kill cancer cells. For example, bispecific antibodies that link CD3 engagement on T cells with various cancer-associated antigens, including CD19, Carcinoembryonic antigen (CEA), and HER2, have shown promising and potent anti-cancer activities.<sup>12–14</sup>

Despite the great promise of using antibodies to elicit potent effector functions, the problem of on-target, off-tumor toxicity continues to be a major challenge. For example, some mAb treatments lead to strong side effects due to this type of toxicity, including cutaneous toxicity (cetuximab), cardiotoxicity (trastuzumab), proteinuria and hypertension (bevacizumab), and neuropathic pain (dinutuximab and naxitamab).<sup>15–19</sup> This same type of problem also occurs for mAbs used in other therapeutic applications, such as ADCs and T cell-engaging bispecific antibodies. For example, ADCs directed against CD44v6 (bivatuzumab mertansine) and

**CONTACT** Greg M. Thurber  [gthurber@umich.edu](mailto:gthurber@umich.edu)  University of Michigan, North Campus Research Complex, Building 28, G056W, 2800 Plymouth Rd, Ann Arbor, MI 48109, USA; Peter M. Tessier  [ptessier@umich.edu](mailto:ptessier@umich.edu)  University of Michigan, North Campus Research Complex, Building 10, A179, 2800 Plymouth Rd, Ann Arbor, MI 48109, USA

 Supplemental data for this article can be accessed online at <https://doi.org/10.1080/19420862.2025.2480666>

© 2025 The Author(s). Published with license by Taylor & Francis Group, LLC.

This is an Open Access article distributed under the terms of the Creative Commons Attribution-NonCommercial License (<http://creativecommons.org/licenses/by-nc/4.0/>), which permits unrestricted non-commercial use, distribution, and reproduction in any medium, provided the original work is properly cited. The terms on which this article has been published allow the posting of the Accepted Manuscript in a repository by the author(s) or with their consent.

Nectin-4 (Padcev®) cause severe skin toxicity.<sup>20,21</sup> Moreover, a bispecific T cell engager targeting CD3 and EGFR to treat colorectal cancer cells resulted in cytokine release and damage to EGFR-expressing organs by redirected T cells.<sup>22</sup>

Many creative approaches have been reported for overcoming on-target, off-tumor toxicity issues. For example, reduction of antibody affinity has been successfully used to reduce off-tumor binding for CAR-T cells while maintaining on-tumor cytotoxic activity.<sup>23</sup> CAR-T cells targeting CD38 with ~1000-fold reduced affinity were able to lyse multiple myeloma cells (high CD38 expression) with similar efficiency as its high-affinity counterpart, but only the low-affinity variant spared healthy hematopoietic cells (low CD38 expression). Similarly, a moderate affinity EpCAM targeting antibody showed a larger therapeutic window compared to other higher affinity antibodies that caused acute pancreatitis.<sup>24</sup> A ~40-fold reduction in affinity of an anti-MET ADC resulted in reduced liver toxicity while maintaining similar tumor uptake and efficacy.<sup>25</sup> If a specific Fc-effector function contributes to toxicity but not efficacy, Fc mutations can tailor the effector function to improve the therapeutic window.<sup>26</sup> The approach of reducing antibody affinity has also been coupled with increasing antibody valency to further expand the therapeutic window for bispecific antibodies. For example, avidity-based binding to HER2 using bispecific antibodies with two binding sites for HER2 and one binding site for CD3 resulted in more selective killing of HER2-overexpressing cells for variants with low HER2 affinity relative to those with high HER2 affinity.<sup>14</sup>

A related study aimed at improving the *in vivo* selectivity of bispecific antibody targeting of model cancer cells with two targets (HER2 and EGFR) relative to cells with only one target (HER2) found that reducing both EGFR antibody avidity (i.e., monovalent Fab binding) and affinity for a 1 × 1 HER2/EGFR bispecific antibody (i.e., one Fab specific for HER2 and one Fab specific for EGFR) was necessary to significantly increase targeting selectivity.<sup>27</sup> Moreover, it has also been shown that reducing the affinity of antibody Fc regions for FcγRs can reduce toxicity, such as liver toxicity associated with CD137 antibodies.<sup>28</sup> Finally, a different approach to reduce target engagement on healthy cells is to engineer the Fv or Fc regions of antibodies to preferentially bind to their corresponding targets (i.e., antigen or Fc receptor, respectively) at the reduced pH conditions in the tumor microenvironment, such as pH-dependent binding for 1) the Fab region binding to HER2 or EGFR<sup>29,30</sup> or 2) the Fc region binding to FcγRIIIa.<sup>31</sup>

However, these previous approaches suffer from two key inherent limitations. First, attempts to increase the selectivity of antibody targeting of tumor vs. non-tumor cells typically result in reduced maximal cell-killing activity. Second, approaches that use bispecific antibodies such as T-cell engagers typically use nonstandard antibody formats, which suffer from increased antibody complexity and associated risks related to increased developability and manufacturing challenges.

Here, we report an approach to address both previous limitations, which is summarized in Figure 1a-d. This approach uses two closely related variants of a therapeutic antibody, which are trastuzumab variants in this study. The first IgG variant, which we refer to as the blocking antibody,

maintains high affinity for the target but contains mutations in the Fc region to eliminate effector function, thereby blocking antibody activity on low-expressing cells. The second IgG variant, which has intact Fc effector functions, has affinity-reducing mutations in the Fab regions to reduce antibody binding to cells with low HER2 levels while maintaining binding to cancer cells with high HER2 levels. In some cases, this variant also has mutations in the Fc domain that increase effector function to maintain high activity on cells with high HER2 levels. Here, we demonstrate that the combinations of the two trastuzumab variants enable both high selectivity and effector function activity (ADCC and ADCP) for cells with high HER2 levels relative to those with low HER2 levels.

## Results

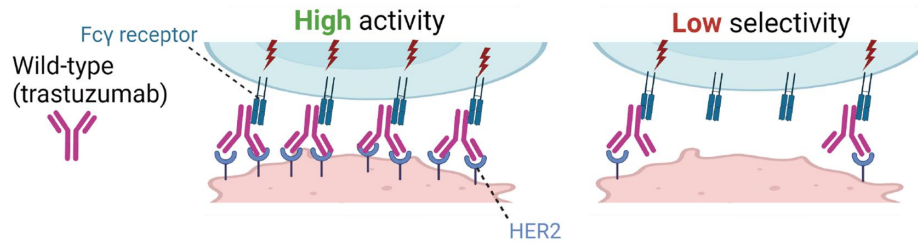
### *Reduced antibody affinity increases the selectivity of activating ADCC reporter cells based on HER2 expression level*

Toward our goal of increasing the selectivity of trastuzumab for cells with high HER2 levels, we first generated affinity-reduced variants by introducing mutations into the heavy chain CDRs and selecting for mutants with reduced affinity using yeast-surface display (see Methods for details). This resulted in the isolation of two variants, namely S4 and S12 (Figure 2a), which we produced as Fab fragments (Figure S1) and characterized in terms of their monovalent affinities (Figure 2b). The S4 Fab variant displayed the weakest affinity ( $K_D > 150$  nM) for high HER2 cells (HCC1954, denoted as HER2<sup>+++</sup>), and its binding levels did not saturate at the highest tested Fab concentration (600 nM). The S12 Fab variant bound with intermediate affinity ( $K_D$  of  $44.1 \pm 6.5$  nM) relative to wildtype (WT) ( $K_D$  of  $9.1 \pm 1.2$  nM).

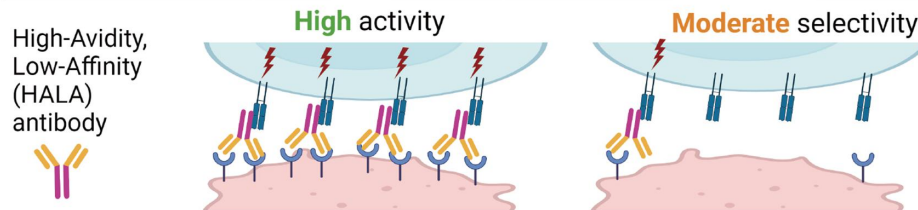
We next reformatted the antibodies as IgGs, produced and purified them (Figure S1), and evaluated their binding to cell lines with high (HER2<sup>+++</sup>) and low (MDA-MB-231, denoted as HER2<sup>+</sup>) HER2 levels (Figure 2c-d). These cell lines have ~1–3 million (HER2<sup>+++</sup>) and ~30,000–40,000 (HER2<sup>+</sup>) receptors per cell, the latter of which is similar to estimates of ~10,000–35,000 HER2 receptors per cell on healthy tissue.<sup>32–37</sup> Interestingly, we observed similar binding of the three IgGs to the HER2<sup>+++</sup> cells ( $EC_{50}$  values of 1.4–2.1 nM; Figure 2c). However, the S4 IgG binds much weaker to the HER2<sup>+</sup> cells ( $EC_{50} > 20$  nM) relative to the S12 ( $EC_{50}$  of  $1.19 \pm 0.19$  nM) and WT ( $EC_{50}$  of  $0.75 \pm 0.15$  nM) antibodies (Figure 2d). These findings suggest that the bivalent nature of the S4 IgG is sufficient to mediate high avidity binding to HER2<sup>+++</sup> cells, but its low intrinsic affinity is insufficient to mediate strong binding to HER2<sup>+</sup> cells. These findings are consistent with our primary goal of generating trastuzumab mutants with high avidity and low affinity, herein referred to as HALA Variants.

To test our hypothesis that the reduced binding of the S4 IgG to HER2<sup>+</sup> cells would increase selectivity of activating ADCC (FcγRIIIa) reporter cells based on HER2 expression, we next conducted experiments using trastuzumab and the two affinity-reduced variants (Figure S2). As expected, we observe little difference between the three antibody variants in terms of activating FcγRIIIa for HER2<sup>+++</sup> cells ( $EC_{50}$  values

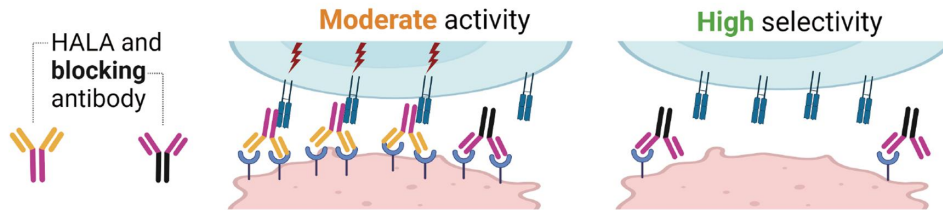
## a. trastuzumab IgG



## b. High-Avidity, Low-Affinity (HALA) trastuzumab IgG variant



## c. HALA IgG and blocking (effectorless) trastuzumab IgG variant



## d. Fc-effector enhanced HALA IgG and blocking IgG

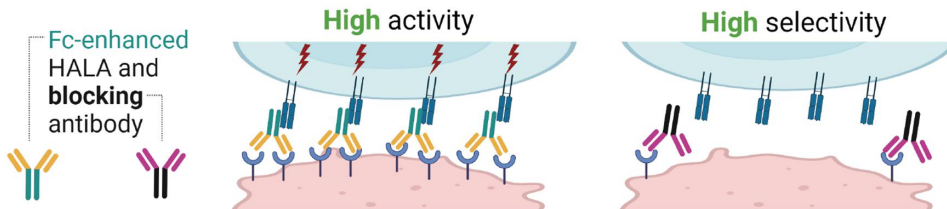


**Figure 1.** Proposed strategy to increase the selectivity of antibody-mediated effector function for target cells with elevated antigen expression using mixtures of engineered antibodies. (a) Wild-type trastuzumab, which has high affinity for its antigen (HER2), binds strongly to cells with either high (HER2<sup>+++</sup>) or low (HER2<sup>+</sup>) levels of antigen, and is expected to mediate relatively high effector function in both cases. This is expected to result in a relatively low effector function ratio for cells with high HER2 levels versus those with low HER2 levels. (b) An engineered version of trastuzumab, namely a high avidity low affinity (HALA) variant, is expected to bind strongly to HER2<sup>+++</sup> cells and weakly to HER2<sup>+</sup> cells. This is expected to result in an increase in the effector function ratio, which is primarily due to reduced effector function on HER2<sup>+</sup> cells. (c) A mixture of the HALA antibody and an effectorless version of trastuzumab that has high HER2 affinity but little affinity for activating FcγRs – referred to as a blocking antibody – is expected to result in a high selectivity with moderate effector function. (d) A mixture of the Fc-enhanced HALA antibody and the blocking antibody is expected to result in high effector function and high selectivity. This is posited to be due to both the accumulation of the 1) Fc-enhanced HALA antibody in the synapses involving HER2<sup>+++</sup> cells, which would lead to high effector function, and 2) effectorless (high affinity) trastuzumab antibody in the synapses involving HER2<sup>+</sup> cells, which would lead to high selectivity. Together, the mixture of the Fc-enhanced HALA antibody and effectorless, high-affinity blocking antibody is expected to lead to both high selectivity and high effector function.

1.06 ± 0.34 nM for WT, 1.59 ± 0.35 nM for S12 and 1.51 ± 0.80 nM for S4), while the S4 IgG is the least potent antibody for the HER2<sup>+</sup> cells (EC<sub>50</sub> values 0.27 ± 0.1 nM for WT, >2.5 nM for S12 and >10 nM for S4). The ratio of activity as a function of antibody concentration demonstrates that S4 IgG is most selective for HER2<sup>+++</sup> cells, especially in the concentration range of 0.13–1.3 nM. Relative to WT and S12 IgG, S4 IgG displays statistically significant increases in selectivity for HER2<sup>+++</sup> cells at antibody concentrations of 0.14–1.2 nM (Figure S3).

We also observed similar behavior for Fc-modified versions of the three trastuzumab variants (Figure S2). Five mutations in the C<sub>H</sub>2 and C<sub>H</sub>3 regions, which have been previously reported to increase ADCC activity,<sup>38</sup> were introduced into the trastuzumab variants (herein referred to as enhanced Fc 1 or eFc1), revealing that the three antibodies displayed similar activity for HER2<sup>+++</sup> cells (EC<sub>50</sub> values 0.37 ± 0.19 nM for WT-eFc1, 0.41 ± 0.16 nM for S12-eFc1 and 0.42 ± 0.35 nM for S4-eFc1), while the S4-eFc1 IgG is the least potent for HER2<sup>+</sup> cells (EC<sub>50</sub> values 0.09 ± 0.01 nM for WT-eFc1, 0.12 ± 0.02 nM for

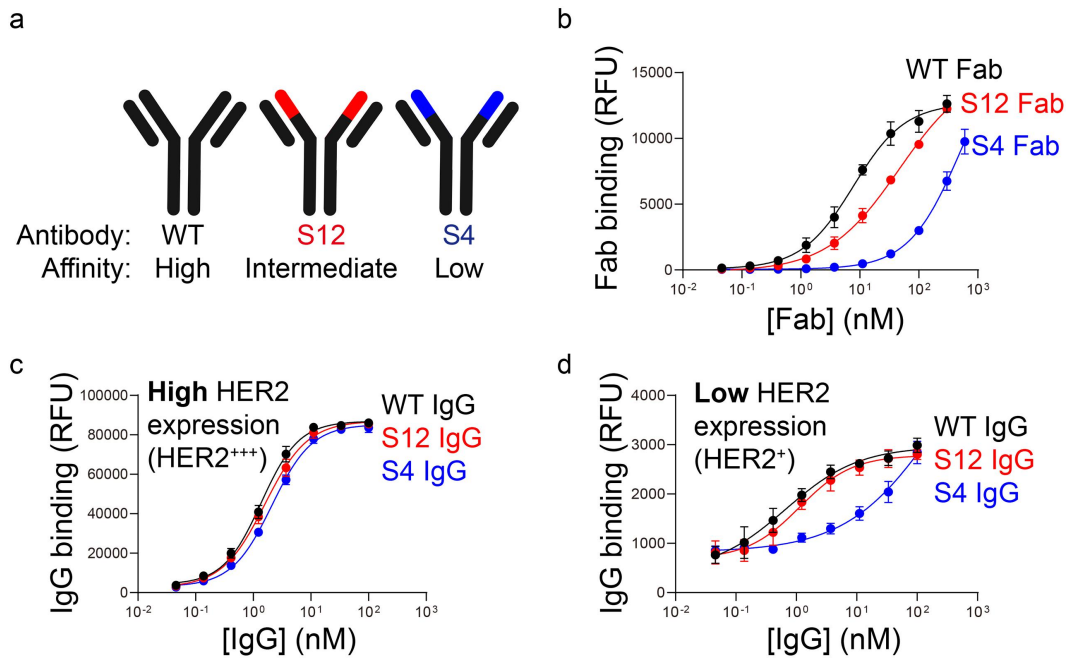


**Figure 2.** Binding affinity measurements for Fab fragments and IgGs corresponding to trastuzumab and its affinity-reduced mutants. (a) The panel of antibodies, which represents wild-type trastuzumab (WT) and two affinity-reduced variants (S12 and S4), was evaluated in the (b) Fab or (c-d) IgG formats for binding to (b-c) HER2<sup>+++</sup> (HCC1954) or (d) HER2<sup>+</sup> (MDA-MB-231) cells. The measurements were performed using flow cytometry, and the error bars are standard errors ( $n = 3$ ).

S12-eFc1 and  $3.49 \pm 1.00$  nM for S4-eFc1). The ratio of activity as a function of antibody concentration demonstrates that S4-eFc1 IgG is most selective for HER2<sup>+++</sup> cells, especially in the concentration range of 0.015–0.14 nM. Relative to WT-eFc1 and S12-eFc1, S4-eFc1 displays statistically significant increases in selectivity for HER2<sup>+++</sup> cells at antibody concentrations of 0.015–3.7 nM (Figure S3).

Finally, we evaluated tradeoffs between the maximum activity and selectivity for activating ADCC reporter cells based on HER2 expression level (Figure S2). For the WT and S12 IgGs, we observed relatively high maximum activities (74–75-fold relative to control), but relatively low maximum selectivities (6.3–7.0 ratios of activity at a given antibody concentration). In these cases, the eFc1 variants further increased maximum activity (98.0–102.3) but reduced selectivity (2–4-fold). In contrast, the S4 IgG showed a similar, albeit slightly lower, maximum activity ( $68.1 \pm 2.9$  relative to 74–75 for WT and S12) but with increased selectivity ( $11.4 \pm 0.3$  relative to 6.3–7.0 for WT and S12). Interestingly, the S4-eFc1 IgG further increased activity ( $94.7 \pm 4.5$ ) without reducing selectivity ( $11.5 \pm 0.6$ ). Collectively, these results demonstrate that the S4-eFc1 IgG has the best combination of maximum activity and selectivity for activating ADCC reporter cells based on HER2 expression level.

#### Mixtures of affinity-reduced and effectorless blocking antibodies maximize ADCC activity and selectivity

We next sought to further improve the selectivity of activation of ADCC reporter cells in a manner dependent on HER2 expression level using mixtures of two trastuzumab variants based on our hypothesis summarized in Figure 1d. Therefore, we first tested the binding of mixtures of two

types of antibodies, namely fluorescently labeled WT trastuzumab or HALA variants with reduced HER2 affinities in the presence of an unlabeled blocking version of trastuzumab that retains high HER2 affinity (WT Fab regions) but is engineered to be effectorless (herein referred to as the “blocker”; Figure 3). For WT:blocker mixtures, WT trastuzumab binding was progressively reduced to both HER2<sup>+++</sup> and HER2<sup>+</sup> cells as the mixture ratio is increased (Figure 3a–b), resulting in maximum HER2<sup>+++</sup>/HER2<sup>+</sup> binding ratios that were similar with and without the blocking antibody (Figure 3c). The ratio values are generally similar to the ratio of expression levels for the two cell lines. However, S12: blocker mixtures resulted in much stronger reduction in binding to HER2<sup>+</sup> cells (Figure 3e) relative to HER2<sup>+++</sup> cells (Figure 3d), resulting in increased binding ratios for the mixtures relative to the single S12 IgG (Figure 3f). For 1:1 mixtures, the increased binding selectivity was statistically significant at S12 IgG concentrations of ~1–10 nM (Figure S4). In contrast, S4:blocker mixtures resulted in strong reductions in binding to both HER2<sup>+++</sup> (Figure 3g) and HER2<sup>+</sup> (Figure 3h) cells, resulting in lower binding ratios than those for the S4 IgG alone (Figure 3i).

After quantifying the binding ratios on cells, we tested the ADCC reporter cell activity for the effector-competent WT, S12, and S4 IgGs in the presence of different ratios of the effectorless blocker (Figure 4). For mixtures with WT trastuzumab IgG, we find that increasing WT IgG:blocker ratios progressively reduces the maximum activity for HER2<sup>+++</sup> cells (Figure 4a). Equimolar (1:1) mixtures result in a maximum activity of 53% relative to the WT IgG alone, while the other mixtures with higher blocker ratios have lower maximum activities (40% for 1:2, 26.7% for 1:4 and 21% for 1:8 antibody:blocker ratio relative to WT IgG alone).



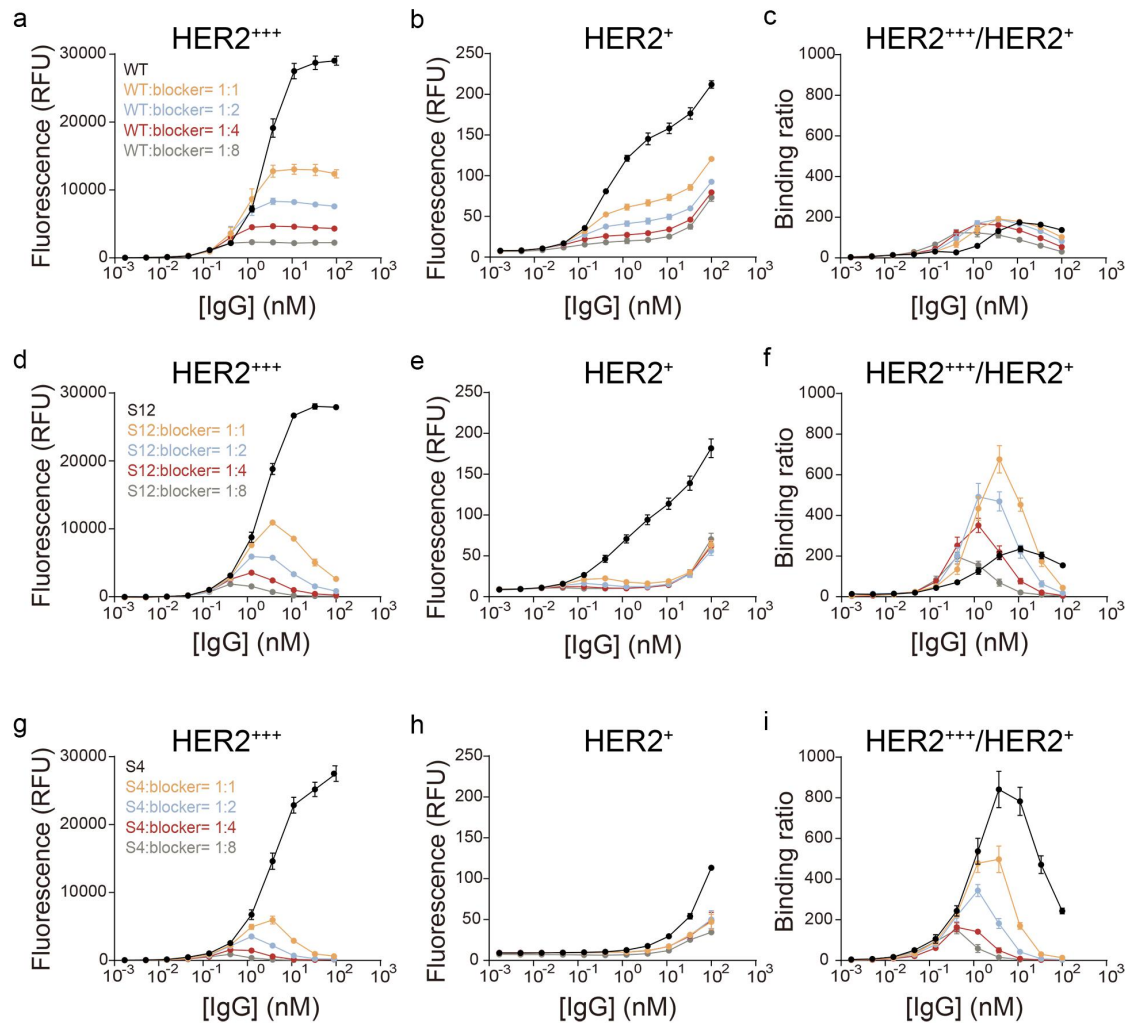


**Figure 3.** Mixtures of HALA and blocker antibody variants of trastuzumab increase the specificity of HALA antibodies for HER2<sup>+++</sup> cells. (a–b) The binding signal for fluorescently labeled wild-type trastuzumab (WT) or HALA variants (S12 and S4) with different ratios of an unlabeled blocking antibody (trastuzumab with Fc mutations that eliminate effector function) corresponding to (a) HER2<sup>+++</sup> and (b) HER2<sup>+</sup> cells, as well as (c) the ratio of binding for fluorescently labeled WT trastuzumab at each antibody mixture concentration for HER2<sup>+++</sup> relative to HER2<sup>+</sup> cells. (d–e) The binding signal for fluorescently labeled S12 with different ratios of the unlabeled blocking antibody corresponding to (d) HER2<sup>+++</sup> and (e) HER2<sup>+</sup> cells, as well as (f) the binding ratio. (g–h) The binding signal for fluorescently labeled S4 with different ratios of the unlabeled blocking antibody corresponding to (g) HER2<sup>+++</sup> and (h) HER2<sup>+</sup> cells, as well as (i) the binding ratio.

A similar trend is observed for the same antibody mixtures on HER2<sup>+</sup> cells, although the overall activation levels are reduced slightly more than those for HER2<sup>+++</sup> cells (Figure 4b). Notably, WT: blocker ratios of 1:4 and 1:8 reduce maximum activation levels to near baseline values. This results in activation ratios that are highest for the 1:4 and 1:8 WT: blocker ratios (Figure 4c).

The S12: blocker (Figure 4d–f) and S4: blocker (Figure 4g–i) results display similar qualitative trends with key quantitative differences relative to the WT: blocker results. First, as observed for the 1:1 WT: blocker ratio (Figure 4a), the 1:1 S12: blocker (Figure 4d) and 1:1 S4: blocker (Figure 4g) ratios also result in the highest activities for HER2<sup>+++</sup> cells compared to antibody mixtures at different ratios (i.e., the lowest blocker levels result in the highest activation). Interestingly, increasing antibody concentrations (even at the same blocker ratio) inhibit activation, including at concentrations >10 nM for S12 mixtures and >3 nM for S4 mixtures. Second, 1:1 S12: blocker (Figure 4e) and 1:1 S4: blocker (Figure 4h) mixtures are sufficient to eliminate activity on HER2<sup>+</sup> cells,

which is unique relative to the behavior observed for the WT: blocker mixtures. Third, the low activity of the 1:1 S12: blocker and 1:1 S4: blocker mixtures for HER2<sup>+</sup> cells leads to higher selectivity, as judged by the HER2<sup>+++</sup>/HER2<sup>+</sup> ratios at each antibody concentration, including maximum values of 36 for S12 mixtures and 30 for S4 mixtures relative to 10.5 for WT mixtures (Figure 4f,i). Fourth, the increased selectivity of S12: blocker mixtures relative to S12 alone was observed at a broad antibody concentration range (statistically significant differences at 0.4–100 nM), while the corresponding S4: blocker mixtures displayed increased selectivity at a smaller range of concentrations (statistically significant differences at 0.3–4 nM; Figure S5).

We next evaluated tradeoffs between maximal activity and selectivity as a function of HER2 expression level (Figure 4j–l). For the WT: blocker mixtures, the maximum activity was strongly reduced as the antibody ratio was increased, while the selectivity only modestly increased and was maximal at the ratios corresponding to the lowest maximal activity (1:8 and 1:4 WT: blocker ratios; Figure 4j). In contrast, the S12: blocker

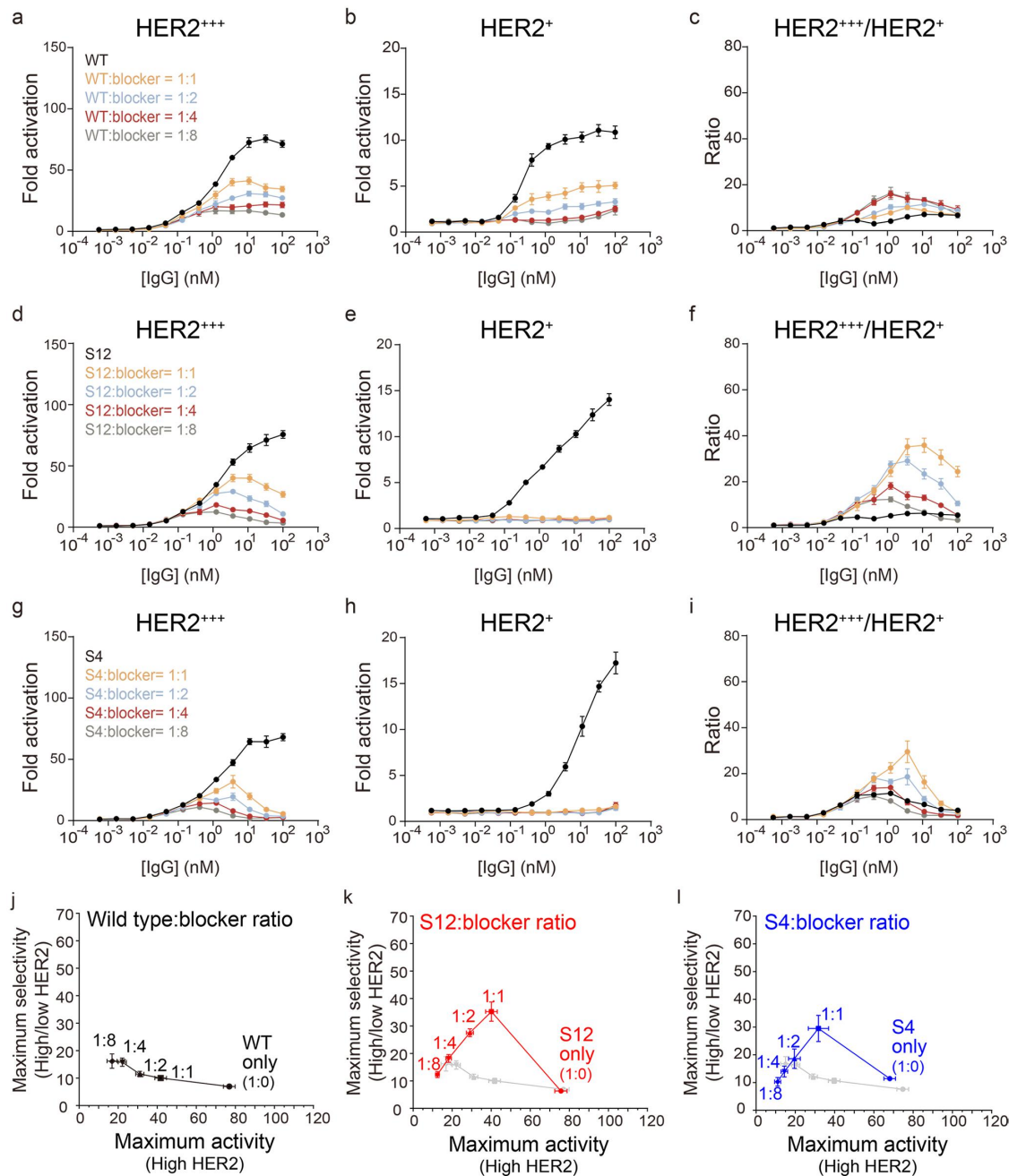


**Figure 4.** Mixtures of HALA and blocker antibody variants of trastuzumab increase the selectivity for activating ADCC reporter cells based on the level of HER2 expression. (a-b) The fold activation of FcγRIIIa (ADCC reporter cells) for mixtures of wild-type trastuzumab (WT) and different ratios of a blocking antibody (trastuzumab with Fc mutations that eliminate effector function) corresponding to (a) HER2<sup>+++</sup> and (b) HER2<sup>+</sup> cells, as well as (c) the ratio of HER2<sup>+++</sup>/HER2<sup>+</sup> activities. (d-e) The fold activation for mixtures of S12 with different ratios of the blocking antibody corresponding to (d) HER2<sup>+++</sup> and (e) HER2<sup>+</sup> cells, as well as (f) the ratio of activities. (g-h) The fold activation for mixtures of S4 with different ratios of the blocking antibody corresponding to (g) HER2<sup>+++</sup> and (h) HER2<sup>+</sup> cells, as well as (i) the ratio of activities. (j-l) Comparison of the maximum activities relative to the maximum selectivities for (j) WT: blocker mixtures, (k) S12: blocker mixtures, and (l) S4: blocker mixtures. In (a-l), the data are averages of three independent experiments, and the error bars are standard errors. In (k-l), the gray data and line correspond to the WT: blocker data shown in (j).

and S4: blocker mixtures displayed maximal selectivities at ratios with intermediate maximal activity (1:1 ratios; Figure 4k,l). At high S12: blocker and S4: blocker ratios (1:8 and 1:4), the mixtures displayed reduced selectivity along with low maximal activity.

The antibody mixtures significantly improved the selectivity of effector function relative to a single antibody, but the maximum activity was reduced. In an attempt to achieve high maximum activity while maintaining or improving the

selectivity of the antibody mixtures for activating ADCC reporter cells based on HER2 expression levels, we next evaluated mixtures using antibodies with enhanced Fc regions (Figure 5). The WT-eFc1 antibody displayed ~35% higher maximal activity for HER2<sup>+++</sup> cells (Figure 5a) relative to the non-enhanced WT antibody (Figure 4a), and this activity was progressively reduced as blocker ratio increased (Figure 5a). This resulted in ~60% reduction in maximum activity at the highest blocker ratio (1:8), which is a smaller

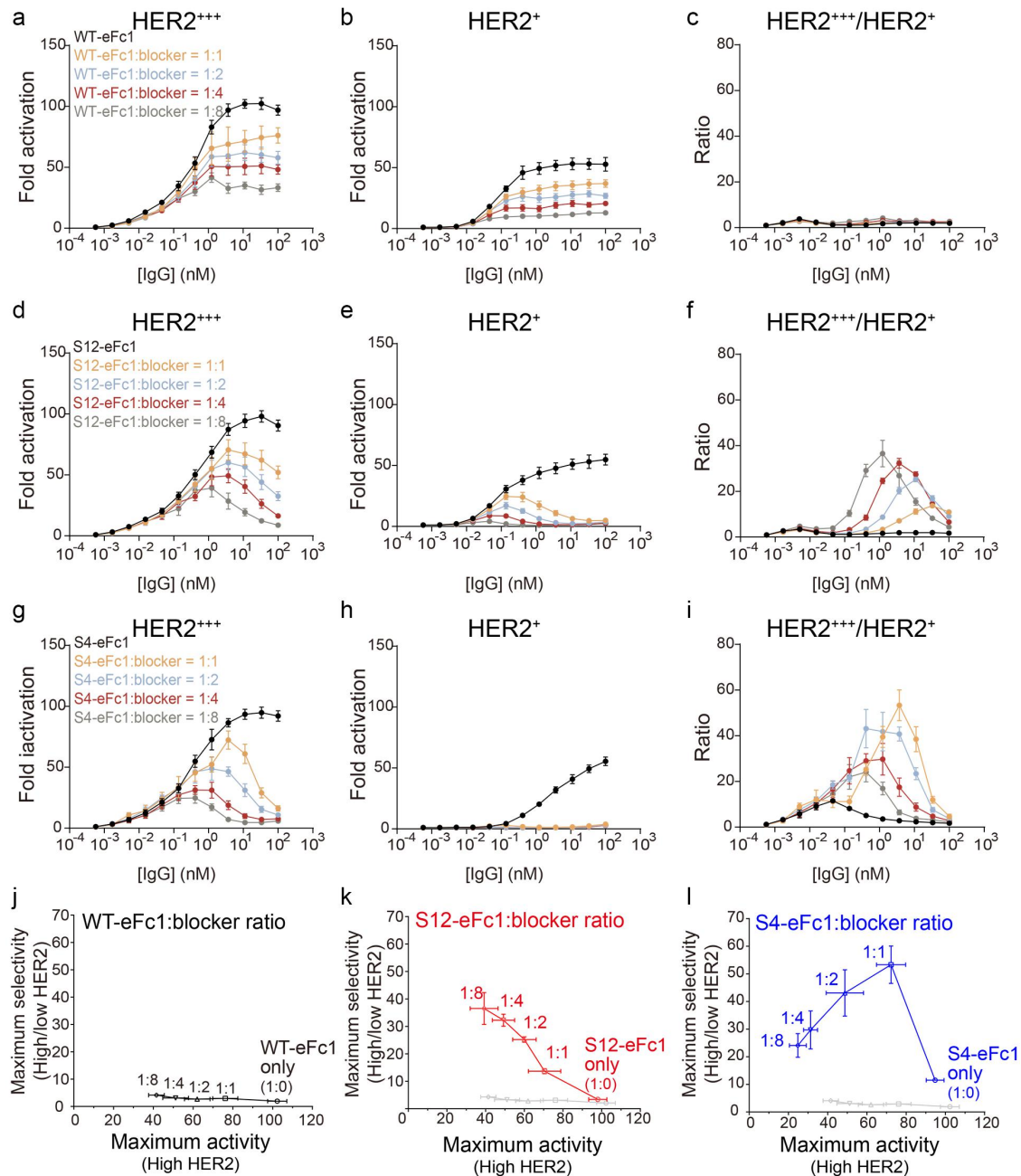


**Figure 5.** Mixtures of HALA antibodies with enhanced Fc $\gamma$ RIIIa affinity and blocking antibodies maximize activity and selectivity while minimizing tradeoffs. (a-b) The fold activation of Fc $\gamma$ RIIIa (ADCC reporter cells) for mixtures of wild-type trastuzumab with enhanced Fc1 (wt-eFc1) and different ratios of a blocking antibody corresponding to (a) HER2<sup>+++</sup> and (b) HER2<sup>+</sup> cells, as well as (c) the ratio of HER2<sup>+++</sup>/HER2<sup>+</sup> activities. (d-e) The fold activation for mixtures of S12-eFc1 with different ratios of the blocking antibody corresponding to (d) HER2<sup>+++</sup> and (e) HER2<sup>+</sup> cells, as well as (f) the ratio of activities. (g-h) The fold activation for mixtures of S4-eFc1 with different ratios of the blocking antibody corresponding to (g) HER2<sup>+++</sup> and (h) HER2<sup>+</sup> cells, as well as (i) the ratio of activities. (j-l) Comparison of the maximum activities relative to the maximum selectivities for (j) wt-eFc1: blocker mixtures, (k) S12-eFc1: blocker mixtures and (l) S4-eFc1: blocker mixtures. In (a-l), the data are averages of three independent experiments, and the error bars are standard errors. In (k-l), the gray data and line correspond to the wt-eFc1: blocker data shown in (j).

reduction than that observed for the corresponding non-enhanced 1:8 WT: blocker mixtures (~80% reduction; Figure 5a). However, the WT-eFc1 antibody also displayed relatively high maximal activity on HER2<sup>+</sup> cells, and this activity was progressively reduced as the blocker ratio was increased (Figure 5a). This resulted in ~75% reduction in activity at the highest blocker ratio (1:8), which is also a smaller reduction than that observed for the non-enhanced 1:8 WT: blocker mixtures (~85% reduction; Figure 4a). This modest ability of the blocking antibody to

reduce activity on HER2<sup>+</sup> cells results in low selectivity, including a maximal HER2<sup>+++</sup>/HER2<sup>+</sup> activation ratio of 16 for WT-eFc1: blocker mixtures (Figure 5c).

In contrast, the S12-eFc1: blocker and S4-eFc1: blocker mixtures displayed unique patterns of behavior (Figure 5d-i). For the S12-eFc1: blocker mixtures, increasing antibody ratios led to some reduction in maximal activity on HER2<sup>+++</sup> cells, including a ~60% reduction of maximum activity for the highest antibody ratio (1:8; Figure 5d), which is similar to that observed for the WT-eFc1: blocker mixtures (Figure 5a).



However, the maximum activity with the blocker is similar to the WT antibody alone (Figure S2). High antibody concentrations progressively reduce activity, as observed for the corresponding non-enhanced mixtures (Figure 4d), at concentrations >3–10 nM for the different S12-eFc1 mixtures (Figure 5d). Notably, the S12-eFc1:blocker mixtures were unable to fully inhibit activity on HER2<sup>+</sup> cells except at the highest ratios (1:8 and 1:4; Figure 5e), which is unique relative to the non-enhanced S12:blocker mixtures (Figure 4e). This results in maximal selectivity at the highest antibody ratios for the S12-eFc1:blocker mixtures (1:8 and 1:4; Figure 5f), which is different than the optimal antibody ratio (1:1) for the non-enhanced S12:blocker mixtures (Figure 4f). However, even at a suboptimal S12-eFc1:blocker ratio of 1:1, we observed statistically significant increases in selectivity relative to the corresponding selectivity for S12-eFc1 (0.4–100 nM for the 1:1 mixtures; Figure S6).

For the S4-eFc1:blocker mixtures, we observe higher maximal activities for HER2<sup>+++</sup> cells (Figure 5g) than that for the corresponding non-enhanced S4:blocker mixtures (Figure 4g). Notably, the S4-eFc1:blocker mixtures do not show activity on HER2<sup>+</sup> cells (Figure 5h), as also observed for S4:blocker mixtures (Figure 4h), which results in increased selectivities for the S4-eFc1:blocker mixtures (Figure 5i) relative to S4:blocker mixtures (Figure 4i). Moreover, statistically significant increases in selectivity of S4-eFc1:blocker mixtures relative to S4-eFc1 alone were observed at a relatively broad range of antibody concentrations (0.4–33 nM for 1:1 mixtures; Figure S6).

Notably, the tradeoffs between maximal activity and selectivity displayed several unique patterns of behavior for the enhanced Fc variants (Figure 5j–l) relative to their WT counterparts (Figure 4j–l). For the WT-eFc1:blocker mixtures, the maximum activity was strongly reduced as the antibody: blocker ratio was increased, while the selectivity was largely unchanged (Figure 5j). In comparison, the WT Fc variants displayed lower maximal activity with modestly higher selectivity (Figure 4j). The maximal activity of the S12-eFc1:blocker mixtures was also significantly reduced as the antibody: blocker ratio increased, but the selectivity progressively increased (Figure 5k). This resulted in the maximum selectivities at the highest S12-eFc1:blocker ratios (1:4 and 1:8, which were not statistically different), while an intermediate antibody ratio was optimal for the S12:blocker mixtures (1:1; Figure 4k). Notably, the maximum activity (39 for 1:8 S12-eFc1:blocker and 40 for 1:1 S12:blocker) and selectivity (40 for 1:8 S12-eFc1: blocker and 35 for 1:1 S12:blocker) for the two different mixtures was similar. Finally, the maximum activity of the S4-eFc1: blocker mixtures was reduced as the antibody ratio increased, with maximum selectivity at 1:1 and 1:2 antibody ratios (not statistically different; Figure 5l), which is higher than the corresponding S4:blocker mixtures (Figure 4l). Importantly, the 1:1 S4-eFc1:blocker mixture resulted in higher maximum activity and selectivity relative to the corresponding non-enhanced mixtures, including an activity of 72-fold induction for 1:1 S4-eFc1:blocker versus 29-fold for 1:1 S4:blocker and a selectivity ratio of 53 for 1:1 S4-eFc1:blocker versus 32 for 1:1 S4:blocker. Overall, the 1:1 S4-eFc1:blocker mixture was able to achieve high activity (72-fold induction; Figure 5l) that was

similar to the maximum activation of the ADCC reporter cells for any of the non-Fc enhanced antibodies (71- to 78-fold induction for WT, S12, and S4; Figure S2) while achieving a 53-fold selectivity compared to the lower (6- to 11-fold) selectivity observed when only modifying the Fab affinity (WT, S12, or S4 alone; Figure 4).

We next tested three additional questions related to our findings. First, do our findings translate to authentic ADCC activity and not simply the activation of FcγRIIIa using ADCC reporter cells? Second, do our findings translate to additional cancer cell lines with either high or low HER2 expression? Third, do we observe similar findings for different allotypes of FcγRIIIa? To test these questions, we evaluated ADCC activity for S4-eFc1 in the presence and absence of the blocking antibody (1:1 ratio) using two HER2<sup>+++</sup> cell lines, namely HCC1954 (~1–3 million receptors per cell) and NCI-N87 (~1–2 million receptors per cell),<sup>35,39</sup> and two HER2<sup>+</sup> cell lines, namely MDA-MB-231 (~30,000–40,000 receptors per cell) and CAPAN-1 (~15,000–20,000 receptors per cell),<sup>40,41</sup> with peripheral blood mononuclear cells (PBMCs) of different allotypes (Figure 6). Notably, we observe a strong decrease in ADCC activity (i.e., target cell lysis) in the presence of the blocking antibody for both cell lines with low HER2 expression, but not for both cell lines with high HER2 expression (Figure 6a–b). These results were similar for both FcγRIIIa allotypes (VV and FF at position 158) and resulted in increased HER2<sup>+++</sup>/HER2<sup>+</sup> lysis ratios (Figure 6c). Overall, these findings highlight that the S4-eFc1:blocker mixture is able to increase the selectivity of ADCC based on the HER2 expression across different cell lines and allotypes.

### **Engineered antibody mixtures also maximize activity and selectivity for antibody-dependent cellular phagocytosis**

Our finding that mixtures of engineered antibodies could significantly improve ADCC selectivity while maintaining high maximum activity motivated us to test if this is also possible to accomplish for a second effector function, namely ADCP. Interestingly, we observed that the effector-competent IgGs (WT, S12 and S4) – in the absence of a blocking antibody – selectively displayed high ADCP reporter cell activity with HER2<sup>+++</sup> cells but not HER2<sup>+</sup> cells (Figure S7). Moreover, we observed similar levels of ADCP reporter signal on HER2<sup>+++</sup> cells when using equivalent IgGs with eFc1 mutations, while also observing a lack of ADCP signal with HER2<sup>+</sup> cells (Figure S8). However, when using a different set of previously reported mutations in the Fc region to enhance effector function,<sup>42</sup> which we herein denote as eFc2, we observed ~3× greater maximum ADCP signaling activity on HER2<sup>+++</sup> cells as well as weaker but significant activity on HER2<sup>+</sup> cells (Figure S7). For the WT-eFc2 and S12-eFc2 IgGs, this resulted in much lower activation ratios relative to the equivalent antibodies with WT Fc regions. However, the maximum ratio for the S4-eFc2 IgG was larger than the equivalent antibody with a WT Fc region. The S4-eFc2 IgG displayed statistically higher ADCP receptor selectivity for HER2<sup>+++</sup> cells at antibody concentrations of 0.015–3.7 nM relative to WT-eFc2 and 0.046–3.7 nM relative to S12-eFc2 (Figure S9).



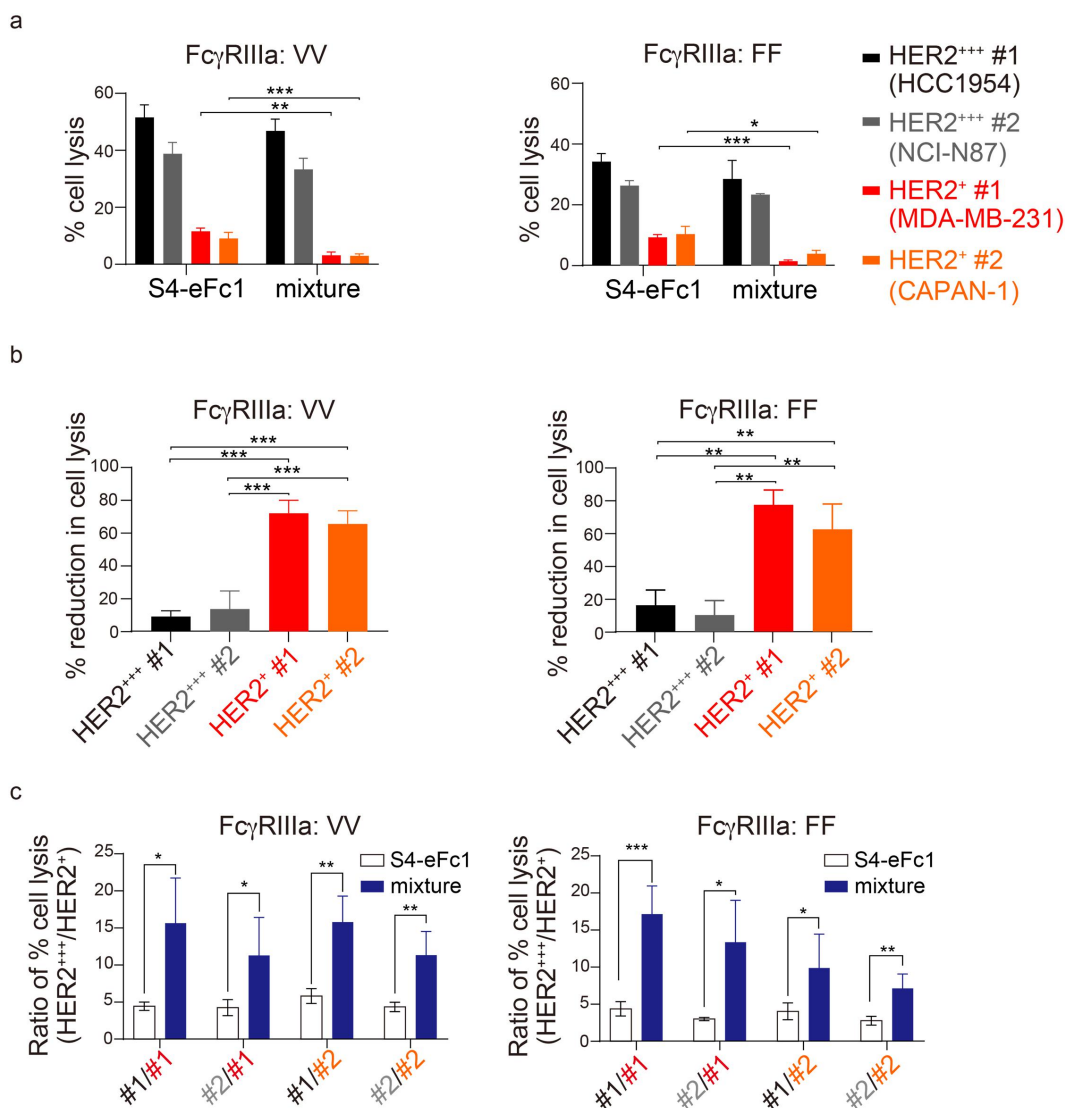


**Figure 6.** Mixtures of HALA antibodies improve the selectivity of ADCC based on HER2 expression level. (a) The percentage of cancer cells lysed for S4-eFc1 (10 nM) alone and with a 1:1 blocker ratio for cell lines with different HER2 expression levels and effector cells with different FcγRIIIa allotypes. (b) The percentage reduction of cancer cell lysis corresponding to the results in (a). (c) The ratio of the percent lysis of cancer cells corresponding to those with high HER2 expression relative to low HER2 expression. In (a-c), the data are averages of two independent experiments, and the error bars are standard deviations.

We next tested if the selectivity of the eFc2 antibodies for activating the ADCP reporter cells could be increased by combining them with an effectorless blocking antibody similar to ADCC activity (Figure 7). For WT-eFc2:blocker mixtures, the maximum activity was modestly impacted for HER2<sup>+++</sup> cells (Figure 7a) but strongly reduced for HER2<sup>+</sup> cells (Figure 7b), which resulted in activation ratios that were much larger than those for WT-eFc2 IgG alone (Figure 7c). The highest selectivity for the WT-eFc2:blocker mixtures was observed at a ratio of 1:8, which improved the selectivity by 10-fold relative to WT-eFc2 IgG alone while modestly reducing the maximum activity for HER2<sup>+++</sup> cells by 28%. Moreover, the increased selectivity of WT-eFc2:blocker mixtures relative to WT IgG alone was observed at a broad antibody concentration range (statistically significant differences at 0.1–100 nM for 1:1 mixtures; Figure S10).

The results for the S12-eFc2 and S4-eFc2 mixtures showed similar qualitative trends but also important differences

relative to the WT-eFc2 mixtures (Figure 7d-i). Both of the affinity-reduced antibodies displayed similar maximum activation in the presence of a blocking antibody for HER2<sup>+++</sup> cells – especially at low S12:blocker and S4:blocker ratios (Figure 7d,g) – while largely eliminating activity on HER2<sup>+</sup> cells (Figure 7e,h). This results in relatively high maximum activation ratios (Figure 7f,i), especially for S4-eFc2 mixtures. The increased selectivity of S12-eFc2 and S4-eFc2 antibodies in the presence of a blocker was observed at a broad antibody concentration range (statistically significant differences at 0.1–100 nM for 1:1 S12-eFc2:blocker mixtures and 1–100 nM for 1:1 S4-eFc2:blocker mixtures; Figure S10). A comparison of the maximum activity and selectivity at each IgG:blocker ratio (Figure 7j-l) reveals that the S4-eFc2:blocker mixture at a ratio of 1:2 leads to the optimal combination of high ADCP reporter activity (maximum fold induction of 395 relative to 402 for the S12-eFc2 IgG alone) and selectivity (ratio of 395 relative to 21 for the S12-eFc2 IgG alone). However, the maximal activity

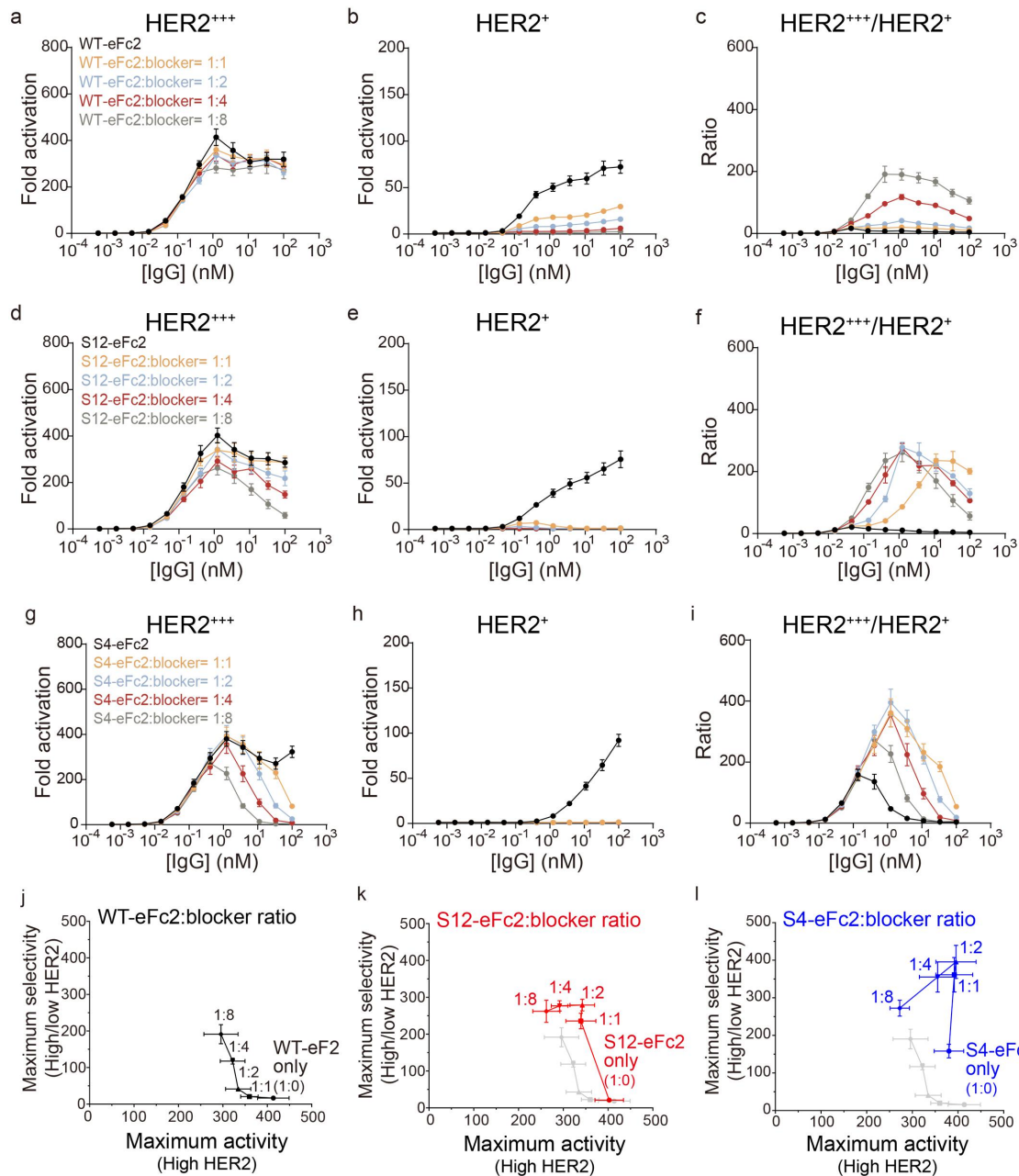


**Figure 7.** Mixtures of HALA antibodies with enhanced FcγRIIIa activity and blocking antibodies maximize activity and selectivity while minimizing tradeoffs. (a-b) The fold activation of FcγRIIIa (ADCP reporter cells) for mixtures of wild-type trastuzumab with enhanced Fc2 (wt-eFc2) and different ratios of a blocking antibody corresponding to (a) HER2<sup>+++</sup> and (b) HER2<sup>+</sup> cells, as well as (c) the ratio of HER2<sup>+++</sup>/HER2<sup>+</sup> activities. (d-e) The fold activation for mixtures of S12-eFc2 with different ratios of the blocking antibody corresponding to (d) HER2<sup>+++</sup> and (e) HER2<sup>+</sup> cells, as well as (f) the ratio of activities. (g-h) The fold activation for mixtures of S4-eFc2 with different ratios of the blocking antibody corresponding to (g) HER2<sup>+++</sup> and (h) HER2<sup>+</sup> cells, as well as (i) the ratio of activities. (j-l) Comparison of the maximum activities relative to the maximum selectivities for (j) wt-eFc2: blocker mixtures, (k) S12-eFc2: blocker mixtures and (l) S4-eFc2: blocker mixtures. In (a-l), the data are averages of three independent experiments, and the error bars are standard errors. In (k-l), the gray data and line correspond to the wt-eFc2: blocker data shown in (j).

and selectivity for the 1:2 S4-eFc2: blocker ratio is not statistically different than the corresponding values for both properties for the 1:1 and 1:4 ratios, although the maximum activity for the 1:2 S4-eFc2: blocker ratio is statistically larger than that for the 1:4 ratio while the maximum selectivity for the 1:2 ratio is statistically larger than that for the 1:1 ratio. Overall, the combination of a blocker antibody with the S4-eFc2 antibody was able to increase both the maximum ADCP reporter activity (395-fold) and selectivity (396-fold; Figure 7) relative to any of the antibodies alone (105-fold activity and 105-fold selectivity; Figure S7)

Similar to the ADCC analysis in Figure 6, we also evaluated whether our findings for the ADCP reporter cells translate to authentic ADCP activity, including for different cancer cell lines and FcγRIIIa allotypes (Figure 8). To address these questions, we evaluated ADCP activity for S4-eFc2 in the presence and absence of blocker (1:1 ratio) using two HER2<sup>+++</sup> (HCC1954 and NCI-N87) and two HER2<sup>+</sup> (MDA-MB-231 and CAPAN-1) cell lines for two FcγRIIIa allotypes (HH and RR at position 131). Notably, we observed almost complete blocking in ADCP activity (i.e., target cell phagocytosis)

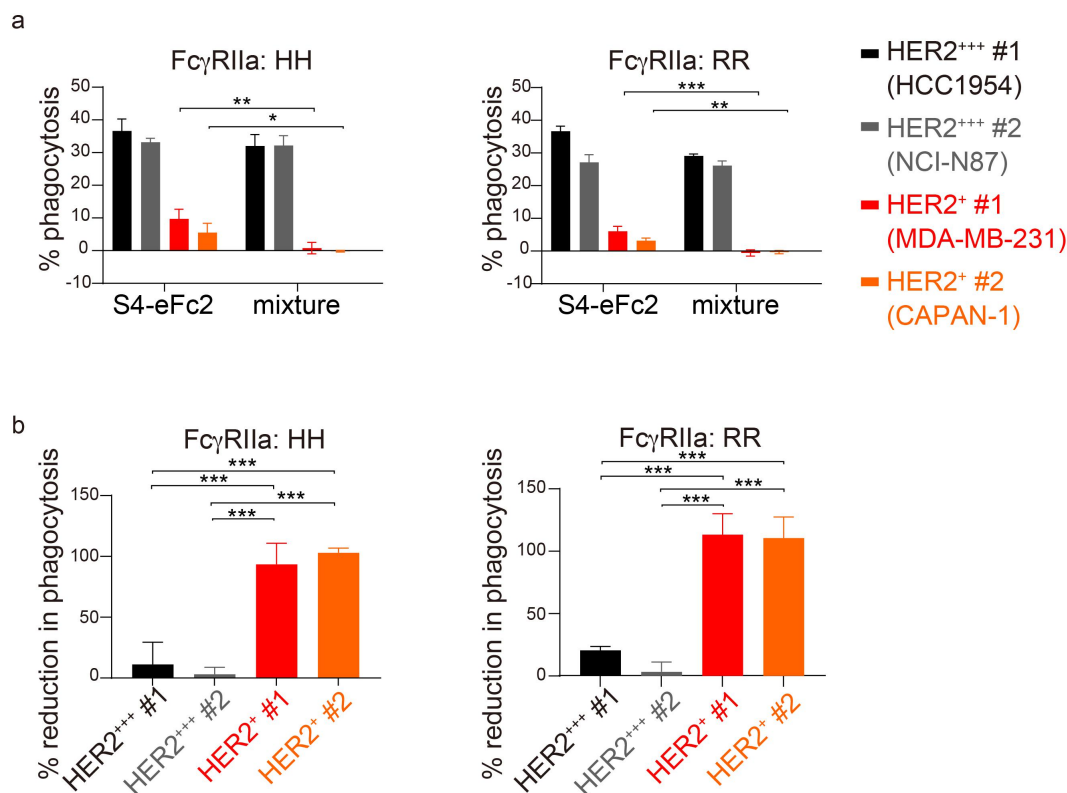


**Figure 8.** Mixtures of HALA antibodies improve the selectivity of ADCP based on HER2 expression level. (a) The percentage of cancer cell phagocytosed for S4-eFc2 (10 nM) alone and with a 1:1 blocker ratio for cell lines with different HER2 expression levels and effector cells with different FcγRIIIa allotypes. (b) The percentage reduction of cancer cell phagocytosis corresponding to the results in (a). In (a-b), the data are averages of two independent experiments, and the error bars are standard deviations.

in the presence of the blocking antibody for both cell lines with low HER2 expression, while we observed little blocking for both cell lines with high HER2 expression (Figure 8a-b). These findings highlight that the S4-eFc2: blocker mixture is able to increase the selectivity of ADCP based on the HER2 expression level across different cell lines and FcγRIIIa allotypes.

## Discussion

Achieving high activity in target tissues while minimizing toxicity-associated activity in healthy tissues is one of the paramount design features of biologics, particularly regarding powerful immune mediation through Fc-effector function. In this work, we used combinations of blocker antibodies and therapeutically active antibodies, the latter of which were engineered with variable Fab and Fc affinities to improve the activity and selectivity of these agents. By both reducing the Fab affinity and increasing the Fc affinity of the effector-competent antibody, we were able to achieve maximum effector function while dramatically improving the selectivity, which could not be achieved by modulating the Fab and/or Fc affinity of a single antibody alone.

One of the most interesting findings in our work is the interplay between the HALA Fab affinity for HER2 and its corresponding Fc affinity for Fcγ receptors in mediating effector function. The ADCC selectivity for the mixtures with HALA antibodies containing WT Fc regions (Figure 4) was similar to the binding specificity to cancer cells measured in the absence of FcγR-expressing effector cells (Figure 3). We posit this is

because the affinities of human IgG1 Fc for FcγRIIIa (CD16a) are relatively weak [ $\sim 400$  nM (V158) and  $1100$  nM (F158)]<sup>10</sup> and thus have little impact on antibody binding in the synapse or the resulting effector function. However, when the Fab affinity of the antibody was reduced, we observed a disconnect between selectivity in the presence and absence of effector reporter cells. For example, the ADCC selectivity of S12-eFc1 was reduced due to increased ADCC activity on HER2<sup>+</sup> cells in the absence of effector cells (Figure 3e). We posit this is because the increased affinity of eFc1 for FcγRIIIa [ $\sim 90$  nM (V158) and  $\sim 160$  nM (F158)] – coupled with the intermediate affinity of S12 for HER2 ( $\sim 45$  nM) – is sufficient to mediate antibody binding in the synapse and increase ADCC activity, thereby reducing selectivity. This is a type of heterotypic avidity, where high-affinity Fc binding to the effector cell aids the binding of the lower affinity Fab arm on the cancer cells, allowing it to out-compete the higher Fab affinity of the blocking antibody that lacks Fc binding and therefore an avidity effect. In contrast, we observe that S4-eFc1 maintains high ADCC selectivity (Figure 5i), which we expect is because its affinity for HER2 ( $>300$  nM) is too low to synergize with the increased affinity of eFc1 for FcγRIIIa, which does not result in antibody binding in the synapse for HER2<sup>+</sup> cells, thereby maintaining high ADCC selectivity. Finally, we observe a similar but weaker effect for ADCP, as S12-eFc2 shows a modest level of ADCP for HER2<sup>+</sup> cells that is not observed for S4-eFc2, which may be due to a similar mechanism via FcγRIIIa (CD32a)-mediated binding of S12-eFc2 in the synapse for HER2<sup>+</sup> cells.

Our findings share several similarities and differences relative to previous studies, which deserve further consideration. First, our finding that reducing antibody affinity increased the binding selectivity and maximum activity for HER2<sup>+++</sup> cells relative to HER2<sup>+</sup> cells is consistent with related bispecific antibody and CAR-T studies involving several different receptors, including HER2, CD38, and EpCAM.<sup>14,23,24</sup> Notably, these studies used relatively large reductions of antibody affinity to achieve increased specificity, such as 150-fold affinity reduction for HER2,<sup>14</sup> 400–500-fold affinity reduction for EpCAM,<sup>24</sup> and 1000-fold affinity reduction for CD38.<sup>23</sup> In contrast, our approach only requires relatively modest reductions in affinity, such as ~5-fold for S12 IgG and ~30-fold for S4 IgG. In some of the former studies, the impact of reducing affinity to increase specificity generally also reduced maximum activity. For example, for bispecific antibodies targeting HER2, lower affinity led to 30% to 50% reduced activity.<sup>14</sup> In contrast, our optimized approach using antibody mixtures targeting HER2 with enhanced Fc regions achieves similar maximum ADCC activity (4.4% reduction) and increased maximum ADCP activity (183% increase) relative to trastuzumab monotherapy while increasing selectivity for HER2<sup>+++</sup> cells.

It is also notable that antibody mixtures, including those involving trastuzumab, have been reported previously, but the goals of these former studies were highly dissimilar to those of this study.<sup>43–45</sup> In particular, antibody mixtures have been used to overcome the binding-site barrier and increase antibody penetration into solid tumors.<sup>45</sup> ADCs are typically administered at lower doses than unconjugated IgGs due to the dose-limiting toxicity of the small molecule payload, which has the unfortunate consequence of typically reducing ADC tissue penetration. To overcome this limitation, co-administration of an ADC (ado-trastuzumab emtansine, T-DM1) along with unconjugated trastuzumab improves tumor penetration and results in significantly better efficacy compared to T-DM1 alone.<sup>44</sup> However, it is notable that this approach accomplishes a different goal than the one in our study, as the former approach reduces the amount of bound ADC on both high- and low-expression cells at the outer region of the tumor using the unconjugated, high-affinity antibody to compete for binding and internalization to enable greater penetration of the ADC into the tumor core. In contrast, our approach seeks to fully block low-expression cells while maximizing activity on high-expression cells.

More generally, our findings highlight a powerful approach for reducing toxicities associated with off-tumor targeting, which is not only important for toxicities associated with antibody-mediated effector functions, but also for toxicities associated with other potent therapies.<sup>46–48</sup> For example, ADCs and T cell engagers exert strong anti-tumor effects through specific binding to their target antigens, but off-tumor, on-target toxicities are commonly observed for such therapies.<sup>46,47</sup> Some T cell-activating antibodies, such as the CD137 agonist urelumab, display severe liver toxicity,<sup>48</sup> and the use of bispecific versions of such antibodies to restrict antibody-mediated receptor activation to the tumor microenvironment has improved the therapeutic window of such therapies.<sup>49,50</sup> Nevertheless, we expect that our approach will provide an

attractive alternative for achieving high selectivity for similar applications as conventional bispecific T cell engagers while maintaining the native IgG format of most approved therapeutic antibodies, which is generally more stable, developable, and safer for clinical applications.

## Materials and methods

### Cloning and recombinant antibody expression

For trastuzumab mutants with WT Fc, VH genes were digested with EcoRI-HF (NEB, R3101L), and NheI-HF (NEB, R3131L), VL genes were digested with EcoRI-HF and BsiWI-HF (NEB, R3553L). pTT5 mammalian expression plasmids containing a common human IgG1 heavy or light (kappa) chain framework were digested with appropriate restriction enzymes and treated with calf intestinal alkaline phosphatase (NEB, M0525L). Digested inserts and vectors were analyzed by electrophoresis using a 1% agarose gel, purified by Qiagen Gel Extraction protocol, ligated with T4 ligase (NEB, M0202L), and transformed by heat shock into DH5α *E. coli* cells. Sequences were confirmed by Sanger sequencing. Fab fragments of trastuzumab mutants were similarly cloned into modified pTT5 mammalian expression plasmids containing IgG1 CH1 or CL framework (linked with a His-tag).

For trastuzumab mutants with mutated Fc, enhancing Fc fragments were ordered as gBlocks (IDT) and replaced the WT Fc by overlap PCR. Five mutations (L235V, F243L, R292P, Y300L, and P396L) were introduced for eFc1, three mutations (G236A, S239D, I332E) were introduced as eFc2, and three mutations (L234A, L235A, and P329G) were introduced as effectorless Fc. The new heavy chains were digested with EcoRI-HF (NEB, R3101L) and BamHI-HF (NEB, R3136L) and inserted into pTT5 mammalian expression plasmids.

For IgG and Fab expression, the CHO-3E7 cell line (National Research Council Canada, L-11992) was cultured in 50 ml disposable conical tubes with F17 (Thermo Fisher Scientific, 50591354) media with 4 mM L-glutamine and 0.1% Kolliphor P188. The cultures were incubated at 37°C and 250 rpm. Soluble IgGs were produced via transient transfection (30 ml) using 12.5 µg each of heavy and light chain plasmids mixed with 100 µg polyethylenimine (PEI MAX; Polysciences Inc., 247651). After transfection, 15 mM Glucose, 1.0% Tryptone N1 (TN1; TekniScience, 19553) and 0.5 mM Valproic Acid (VPA; Sigma, P4543) were added to each batch. Six days after transfection, cultures were centrifuged at 3500 × g for 40 min. Supernatants were collected into new tubes.

For IgG purification, 0.5 ml dry volume of Protein A beads (Thermo Fisher Scientific, 20333) per tube was added. Mixtures were gently shaken at 4°C overnight. Protein A beads were then collected by vacuum filter columns (Thermo Fisher Scientific, 89898) and then washed with around 100 ml of phosphate-buffered saline (PBS). Antibodies were then eluted by 1 ml of 0.1 M glycine buffer (pH 3.0) and then was buffer exchanged to 0.1 M acetate (pH 5.0) with Zeba desalting columns (Thermo Fisher Scientific, 89890). For Fab fragments, 0.5 ml dry volume of Ni-NTA beads (Qiagen, 30210) per tube was added. Mixtures were



gently shaken at 4°C overnight. Beads were collected by vacuum filter columns and then washed with around 100 ml of PBS. Fab fragments were washed with 50 mM imidazole and eluted with 1 ml of 100 mM imidazole, then buffer-exchanged to 0.1 M acetate (pH 5.0). After measuring the concentration, IgGs and Fab fragments were aliquoted and stored at -80°C.

IgG and Fab fragments were further purified by preparative size-exclusion chromatography (SEC) using a Shimadzu Prominence semi-prep HPLC System outfitted with an LC-20AT pump, SIL-20AC autosampler, and FRC-10A fraction collector. Proteins were loaded onto an SEC column (Superdex 200 Increase 10/300 GL column; GE, 28990944) and analyzed at 0.75 mL/min using a PBS running buffer with 200 mM arginine (pH 7.4). After purification, IgG and Fab fragments were buffer exchanged into PBS with Zeba desalting columns (Thermo Fisher, 89890), aliquoted, snap frozen, and stored at -80°C.

### **Antibody labeling**

Fab fragments or IgGs were concentrated to ~2 mg/ml in 100 µl PBS in 1.5 ml tubes. Ten microliters of 7.5% sodium bicarbonate (MilliporeSigma, S6014) was added to each tube to adjust pH to 8–8.5. Then, 2 µl of 10 mg/ml Alexa-647 (Fisher Scientific, A37573) was added to each tube. Tubes were put on a shaking plate for 1 h at room temperature. To purify the fluorescently labeled Fab fragments, 850 µL of 10% P6 Biogel (Bio-Rad, 1504130) was added to a costar spin-x tube (Corning, 07-200-387), and spun down at 3500 × g for 1.5 min. The eluent from the bottom of the tube was removed and then ~400 µL more 10% P6 Biogel was added again. Tubes were spun down at 3500 × g for 1.5 min. The eluent from the bottom of the tube was removed and the reaction mixture was added to the top of the column. Tubes were spun down at 3500 × g for 1.5 min. The eluent was collected into a new 1.5 ml tube. The protein concentration and degree of labeling were measured on the nanodrop.

### **Fab affinity measurements**

HCC1954 cells (ATCC, CRL-2338) were cultured in T75 flasks using RPMI 1640 media (Fisher, A1049101) with 10% HI FBS (Fisher, 10082147) and 1% Penicillin-Streptomycin (P/S) (Fisher, 15140122) at 37°C and 5% CO<sub>2</sub>. HCC1954 cells in each T75 were treated with 2.5 ml trypsin (Fisher, 25-300-054). After detaching, 7.5 ml of RPMI 1640 was added and all media were collected in 15 ml tubes. Cells were spun down at 800 × g for 5 min and then rewashed and resuspended by PBS with 0.1% bovine serum albumin (PBSB). Fab fragments were diluted in PBSB as a 3-fold series starting from 1200 nM and added to 96-well U-bottom plates as 100 µl/well. Cells were added as 50,000 cells/well in 100 µL. Plates were then chilled on ice for 4 h. After incubation, cells were washed with PBSB at 2500 × g for 5 min and then resuspended in 100 µL PBSB. Florescent signals were measured by flow cytometry (Bio-Rad Ze5).

### **IgG affinity measurements**

HCC1954 cells were cultured in T75 flasks with RPMI 1640 media, 10% HI FBS and 1% P/S at 37°C and 5% CO<sub>2</sub>. MDA-MB-231 cells were cultured in T75 flasks using DMEM media (Fisher, 11965092) with 10% HI FBS and 1% P/S at 37°C and 5% CO<sub>2</sub>. The cell collection methods are the same as mentioned in the last section. IgGs were diluted in PBSB as a 3-fold series starting from 200 nM and added to 96-well U-bottom plates as 100 µl/well. Cells were added as 50,000 cells/well in 100 µL. Plates were then chilled on ice for 4 h. After incubation, cells were washed with PBSB at 2500 × g for 5 min. Alexa anti-human Fc (Jackson ImmunoResearch, 109-605-190) was diluted with PBSB 300-fold and added to each well as 100 µL. Plates were incubated on ice for 4 min. Then cells were washed with PBSB at 2500 × g for 5 min and then resuspended in 100 µL PBSB. Florescent signals were measured by flow cytometry.

### **IgG competitive binding measurements**

HCC1954 cells and MDA-MB-231 cells were cultured as mentioned in the last section. After detaching, cells were seeded to 96-well flat-bottom plates (Corning, 07-200-90) at 50,000 cells/well and incubated at 37°C and 5% CO<sub>2</sub> overnight. On the second day, fluorescent-labeled antibodies were diluted as a 3-fold series starting from 100 nM, and blocking antibodies were added as required. One hundred microliters of diluted antibody was added to each well and incubated at 37°C and 5% CO<sub>2</sub> for 6 h. After incubation, cells were detached by trypsin and washed with PBS. Florescent signals were then measured by flow cytometry.

### **ADCC and ADCP reporter cell assays**

ADCC reporter cells (Invivogen, jktl-nfat-cd16) and ADCP reporter cells (Invivogen, jktl-nfat-cd32) were cultured in IMDM media (Fisher, 12440053) with 10% HI FBS, 1% P/S, and 100 µg/ml Normocin (Invivogen, ant-nr-1). Ten micrograms per milliliter of Blasticidin (Invivogen, ant-bl-05) and 100 µg/ml of Zeocin (Invivogen, ant-zn-05) were added to the growth media for each passage. HCC1954 and MDA-MB-231 cells were seeded to 96-well flat-bottom plates as 50,000 cells/well and incubated at 37°C and 5% CO<sub>2</sub> overnight. On the second day, testing antibodies were diluted as a 3-fold series starting from 100 nM, and blocking antibodies were added as required. Next, 110 µL of the diluted antibody was added to each well and incubated at 37°C and 5% CO<sub>2</sub> for 1 h. The ADCC or ADCP reporter cells were then centrifuged at 300 × g for 5 min. The supernatant was removed and the ADCC or ADCP reporter cells were resuspended in the test medium (IMDM media with 10% HI FBS, 1% P/S). Ninety microliters of ADCC or ADCP reporter cells (0.2 million cells) per well were added and the plates were incubated at 37°C and 5% CO<sub>2</sub> for 6 h. After incubation, 20 µL of co-incubated supernatant was transferred into a white assay plate (Fisher, 720,091). Finally, 50 µL of QUANTI-Luc™ (Invivogen, REPQLC2) was added per well and evaluated immediately with the luminometer measurement. Raw signals were

normalized by the signal of negative controls (mixture of cancer cells and reporter cells without antibodies).

### ADCC assay

PBMCs were purchased from STEMCELL (70025) and cultured in T75 flasks with RPMI 1640 (10% HI FBS). PBMC and target cells were then mixed with an effector (E): tumor (T) ratio of 10:1, along with the indicated concentrations of antibodies at 37°C and 5% CO<sub>2</sub>. After 4 h, the lactate dehydrogenase (LDH) level was measured by CyQUANT Cytotoxicity Assay Kit (Fisher, C20301). The % lysis was calculated as  $(A - B)/(C - B) \times 100$ , where “A” is the background subtracted absorbance value of each test sample, “B” is the background subtracted absorbance value without effector cells (i.e., spontaneous release), and “C” is the background subtracted absorbance value for maximum cell lysis (i.e., after adding lysis buffer to cancer cells without effector cells).

### ADCP assay

PBMCs were purchased from STEMCELL (70025) and were cultured in T75 flasks with RPMI 1640 (10% HI FBS and 1% P/S) for 1 h to allow attachment of the monocytes. Monocytes were then differentiated over 6 d in RPMI 1640 with 100 ng/mL human M-CSF (Fisher, PHC9501), 10% HI FBS, and 1% P/S. Macrophages were labeled with CellTrace Violet (10 μM; Fisher, C34557), and cancer cells were labeled with carboxyfluorescein diacetate succinimidyl ester (CFSE) (10 μM; Fisher, C34554), as described in the manufacturer's protocol. Macrophages and target cells were then mixed with an E:T ratio of 4:1, along with the indicated concentrations of antibodies, and incubated at 37°C and 5% CO<sub>2</sub>. After 4 h, adherent cells were detached with accutase, combined with non-adherent cells, and the fluorescence was evaluated by flow cytometry. The percentage of phagocytosis was calculated as  $100 \times (\# \text{ of double positive cells for CFSE}^+ \text{ and celltrace violet}^+ \text{ cells})/(\# \text{ of CFSE}^+ \text{ cells})$ .

### Acknowledgments

We thank members of the Tessier and Thurber labs for their helpful suggestions.

### Disclosure statement

The authors hold pending patents on combination antibody therapeutics. P.M.T. is a member of the scientific advisory boards for Nabla Bio, Aureka Biotechnologies, Dualitas Therapeutics, and CelineBio. G.M.T. has served on the scientific advisory boards of AstraZeneca/Medimmune, Advanced Proteome Therapeutics, Catalent, Merck, Mersana, and Neoleukin.

### Funding

This work was supported by the Department of Defense [W81XWH-21-1-0039 to P.M.T. and G.M.T.], and the Albert M. Mattocks Chair (to P.M.T.).

### ORCID

Alec A. Desai  <http://orcid.org/0000-0002-8322-7096>  
Greg M. Thurber  <http://orcid.org/0000-0001-7570-2080>  
Peter M. Tessier  <http://orcid.org/0000-0002-3220-007X>

### Author contributions

P.M.T. and G.M.T. conceived the project. T.W. and A.D. performed the experiments. P.M.T., T.W. and G.M.T. wrote the paper with feedback from the coauthors.

### References

- Delidakis G, Kim JE, George K, Georgiou G. Improving antibody therapeutics by manipulating the Fc domain: immunological and structural considerations. *Annu Rev Biomed Eng.* 2022;24(1):249–274. doi: [10.1146/annurev-bioeng-082721-024500](https://doi.org/10.1146/annurev-bioeng-082721-024500).
- Kurai J, Chikumi H, Hashimoto K, Yamaguchi K, Yamasaki A, Sako T, Touge H, Makino H, Takata M, Miyata M, et al. Antibody-dependent cellular cytotoxicity mediated by cetuximab against lung cancer cell lines. *Clin Cancer Res.* 2007;13(5):1552–1561. doi: [10.1158/1078-0432.CCR-06-1726](https://doi.org/10.1158/1078-0432.CCR-06-1726).
- Manches O, Lui G, Chaperot L, Gressin R, Molens J-P, Jacob M-C, Sotto J-J, Leroux D, Bensa J-C, Plumas J. In vitro mechanisms of action of rituximab on primary non-Hodgkin lymphomas. *Blood.* 2003;101(3):949–954. doi: [10.1182/blood-2002-02-0469](https://doi.org/10.1182/blood-2002-02-0469).
- Carson WE, Parihar R, Lindemann MJ, Personeni N, Dierksheide J, Meropol NJ, Baselga J, Caligiuri MA. Interleukin-2 enhances the natural killer cell response to herceptin-coated Her2/neu-positive breast cancer cells. *Eur J Immunol.* 2001;31(10):3016–3025. doi: [10.1002/1521-4141\(2001010\)31:10<3016::AID-IMMU3016>3.0.CO;2-J](https://doi.org/10.1002/1521-4141(2001010)31:10<3016::AID-IMMU3016>3.0.CO;2-J).
- Clynes RA, Towers TL, Presta LG, Ravetch JV. Inhibitory Fc receptors modulate in vivo cytotoxicity against tumor targets. *Nat Med.* 2000;6(4):443–446. doi: [10.1038/74704](https://doi.org/10.1038/74704).
- Arce Vargas F, Furness AJS, Litchfield K, Joshi K, Rosenthal R, Ghorani E, Solomon I, Lesko MH, Ruef N, Roddie C, et al. Fc effector function contributes to the activity of human anti-CTLA-4 antibodies. *Cancer Cell.* 2018;33(4):649–663 e4. doi: [10.1016/j.ccell.2018.02.010](https://doi.org/10.1016/j.ccell.2018.02.010).
- Overdijk MB, Verploegen S, Bögers M, van Egmond M, van Bueren JJL, Mutis T, Groen RW, Breij E, Martens AC, Bleeker WK, Parren PW, et al. Antibody-mediated phagocytosis contributes to the anti-tumor activity of the therapeutic antibody daratumumab in lymphoma and multiple myeloma. *mAbs.* 2015;7(2):311–321. doi: [10.1080/19420862.2015.1007813](https://doi.org/10.1080/19420862.2015.1007813).
- VanDermeid KR, Elliott MR, Baran AM, Barr PM, Chu CC, Zent CS. Cellular cytotoxicity of next-generation CD20 monoclonal antibodies. *Cancer Immunol Res.* 2018;6(10):1150–1160. doi: [10.1158/2326-6066.CIR-18-0319](https://doi.org/10.1158/2326-6066.CIR-18-0319).
- Bang YJ, Giaccone G, Im SA, Oh DY, Bauer TM, Nordstrom JL, Li H, Chichili GR, Moore PA, Hong S, et al. First-in-human phase 1 study of margetuximab (MGAH22), an Fc-modified chimeric monoclonal antibody, in patients with HER2-positive advanced solid tumors. *Ann Oncol.* 2017;28(4):855–861. doi: [10.1093/annonc/mdx002](https://doi.org/10.1093/annonc/mdx002).
- Nordstrom JL, Gorlatov S, Zhang W, Yang Y, Huang L, Burke S, Li H, Ciccarone V, Zhang T, Stavenhagen J, et al. Anti-tumor activity and toxicokinetics analysis of MGAH22, an anti-HER2 monoclonal antibody with enhanced Fcγ receptor binding properties. *Breast Cancer Res.* 2011;13(6):R123. doi: [10.1186/bcr3069](https://doi.org/10.1186/bcr3069).
- Offidani M, Corvatta L, Morè S, Olivieri A. Belantamab Mafodotin for the treatment of multiple myeloma: an overview of the clinical efficacy and safety. *Drug Des Devel Ther.* 2021;15:2401–2415. doi: [10.2147/DDDT.S267404](https://doi.org/10.2147/DDDT.S267404).

12. Przepiorka D, Ko C-W, Deisseroth A, Yancey CL, Canda-Chacon R, Chiu H-J, Gehrke BJ, Gomez-Broughton C, Kane RC, Kirshner S, et al. FDA approval: Blinatumomab. *Clin Cancer Res.* 2015;21(18):4035–4039. doi: [10.1158/1078-0432.CCR-15-0612](#).
13. Bacac M, Klein C, Umana P. CEA TCB: a novel head-to-tail 2: 1 T cell bispecific antibody for treatment of CEA-positive solid tumors. *Oncoimmunology.* 2016;5(8):e1203498. doi: [10.1080/2162402X.2016.1203498](#).
14. Slaga D, Ellerman D, Lombana TN, Vij R, Li J, Hristopoulos M, Clark R, Johnston J, Shelton A, Mai E, et al. Avidity-based binding to HER2 results in selective killing of HER2-overexpressing cells by anti-HER2/CD3. *Sci Transl Med.* 2018;10(463):eaat5775. doi: [10.1126/scitranslmed.aat5775](#).
15. Holcmann M, Sibilia M. Mechanisms underlying skin disorders induced by EGFR inhibitors. *Mol Cell Oncol.* 2015;2(4):e1004969. doi: [10.1080/23723556.2015.1004969](#).
16. Dempsey N, Rosenthal A, Dabas N, Kropotova Y, Lippman M, Bishopric NH. Trastuzumab-induced cardiotoxicity: a review of clinical risk factors, pharmacologic prevention, and cardiotoxicity of other HER2-directed therapies. *Breast Cancer Res Treat.* 2021;188(1):21–36. doi: [10.1007/s10549-021-06280-x](#).
17. Eremina V, Jefferson JA, Kowalewska J, Hochster H, Haas M, Weisstuch J, Richardson C, Kopp JB, Kabir MG, Backx PH, et al. VEGF inhibition and renal thrombotic microangiopathy. *N Engl J Med.* 2008;358(11):1129–1136. doi: [10.1056/NEJMoa0707330](#).
18. Kushner BH, Cheung IY, Modak S, Basu EM, Roberts SS, Cheung N-K. Humanized 3F8 anti-G D2 monoclonal antibody dosing with granulocyte-macrophage colony-stimulating factor in patients with resistant neuroblastoma. *JAMA Oncol.* 2018;4(12):1729–1735. doi: [10.1001/jamaoncol.2018.4005](#).
19. Mastrangelo S, Rivetti S, Triarico S, Romano A, Attinà G, Maurizi P, Ruggiero A. Mechanisms, characteristics, and treatment of neuropathic pain and peripheral neuropathy associated with Dinutuximab in neuroblastoma patients. *Int J Mol Sci.* 2021;22(23):12648. doi: [10.3390/ijms222312648](#).
20. Rupp U, Schoendorf-Holland E, Eichbaum M, Schuetz F, Lauschner I, Schmidt P, Staab A, Hanft G, Huober J, Sinn H-P, et al. Safety and pharmacokinetics of bivatuzumab mertansine in patients with CD44v6-positive metastatic breast cancer: final results of a phase I study. *Anticancer Drugs.* 2007;18(4):477–485. doi: [10.1097/CAD.0b013e32801403f4](#).
21. Lacouture ME, Patel AB, Rosenberg JE, O'Donnell PH. Management of dermatologic events associated with the nectin-4-directed antibody-drug conjugate Enfortumab Vedotin. *Oncologist.* 2022;27(3):e223–e232. doi: [10.1093/oncolo/oyac001](#).
22. Lutterbuese R, Raum T, Kischel R, Hoffmann P, Mangold S, Rattel B, Friedrich M, Thomas O, Lorenczewski G, Rau D, et al. T cell-engaging BiTE antibodies specific for EGFR potently eliminate KRAS- and braf-mutated colorectal cancer cells. *Proc Natl Acad Sci USA.* 2010;107(28):12605–12610. doi: [10.1073/pnas.1000976107](#).
23. Drent E, Themeli M, Poels R, de Jong-Korlaar R, Yuan H, de Bruijn J, Martens ACM, Zweegman S, van de Donk NWCJ, Groen RWJ, et al. A rational strategy for reducing on-target off-tumor effects of CD38-chimeric antigen receptors by affinity optimization. *Mol Ther.* 2017;25(8):1946–1958. doi: [10.1016/j.ymthe.2017.04.024](#).
24. Munz M, Murr A, Kvesic M, Rau D, Mangold S, Pflanz S, Lumsden J, Volkland J, Fagerberg J, Riethmüller G, et al. Side-by-side analysis of five clinically tested anti-EpCAM monoclonal antibodies. *Cancer Cell Int.* 2010;10(1):44. doi: [10.1186/1475-2867-10-44](#).
25. Datta-Mannan A, Choi H, Jin Z, Liu L, Lu J, Stokell DJ, Murphy AT, Dunn KW, Martinez MM, Feng Y, et al. Reducing target binding affinity improves the therapeutic index of anti-met antibody-drug conjugate in tumor bearing animals. *PLoS One.* 2024;19(4):e0293703. doi: [10.1371/journal.pone.0293703](#).
26. Navid F, Sondel PM, Barfield R, Shulkin BL, Kaufman RA, Allay JA, Gan J, Hutson P, Seo S, Kim K, et al. Phase I trial of a novel anti-GD2 monoclonal antibody, Hu14.18K322A, designed to decrease toxicity in children with refractory or recurrent neuroblastoma. *J Clin Oncol.* 2014;32(14):1445–1452. doi: [10.1200/JCO.2013.50.4423](#).
27. Mazor Y, Sachsenmeier KF, Yang C, Hansen A, Filderman J, Mulgrew K, Wu H, Dall'acqua WF. Enhanced tumor-targeting selectivity by modulating bispecific antibody binding affinity and format valence. *Sci Rep.* 2017;7(1):40098. doi: [10.1038/srep40098](#).
28. Ho SK, Xu Z, Thakur A, Fox M, Tan SS, DiGiammarino E, Zhou L, Sho M, Cairns B, Zhao V, et al. Epitope and Fc-mediated cross-linking, but not high affinity, are critical for antitumor activity of CD137 agonist antibody with reduced liver toxicity. *Mol Cancer Ther.* 2020;19(4):1040–1051. doi: [10.1158/1535-7163.MCT-19-0608](#).
29. Liu X, Tian X, Hao X, Zhang H, Wang K, Wei Z, Wei X, Li Y, Sui J. A cross-reactive pH-dependent EGFR antibody with improved tumor selectivity and penetration obtained by structure-guided engineering. *Mol Ther Oncolytics.* 2022;27:256–269. doi: [10.1016/j.omto.2022.11.001](#).
30. Sulea T, Rohani N, Baardsnes J, Corbeil CR, Deprez C, Cepero-Donates Y, Robert A, Schrag JD, Parat M, Duchesne M, et al. Structure-based engineering of pH-dependent antibody binding for selective targeting of solid-tumor microenvironment. *mAbs.* 2020;12(1):1682866. doi: [10.1080/19420862.2019.1682866](#).
31. Liu Y, Lee AG, Nguyen AW, Maynard JA. An antibody Fc engineered for conditional antibody-dependent cellular cytotoxicity at the low tumor microenvironment pH. *J Biol Chem.* 2022;298(4):101798. doi: [10.1016/j.jbc.2022.101798](#).
32. Khera E, Dong S, Huang H, de Bever L, van Delft FL, Thurber GM. Cellular-resolution imaging of bystander payload tissue penetration from antibody-drug conjugates. *Mol Cancer Ther.* 2022;21(2):310–321. doi: [10.1158/1535-7163.MCT-21-0580](#).
33. Hendriks BS, Klinz SG, Reynolds JG, Espelin CW, Gaddy DF, Wickham TJ. Impact of tumor HER2/ERBB2 expression level on HER2-targeted liposomal doxorubicin-mediated drug delivery: multiple low-affinity interactions lead to a threshold effect. *Mol Cancer Ther.* 2013;12(9):1816–1828. doi: [10.1158/1535-7163.MCT-13-0180](#).
34. Costantini DL, Bateman K, McLarty K, Vallis KA, Reilly RM. Trastuzumab-resistant breast cancer cells remain sensitive to the Auger electron-emitting radiotherapeutic agent <sup>111</sup>In-NLS-Trastuzumab and are radiosensitized by methotrexate. *J Nucl Med.* 2008;49(9):1498–1505. doi: [10.2967/jnumed.108.051771](#).
35. Major M, Nervig CS, Gerland A, Owen SC. Surface-available HER2 levels alone are not indicative of cell response to HER2-targeted antibody-drug conjugate therapies. *Pharmaceutics.* 2024;16(6):752. doi: [10.3390/pharmaceutics16060752](#).
36. Onsum MD, Geretti E, Paragas V, Kudla AJ, Moulis SP, Luus L, Wickham TJ, McDonagh CF, MacBeath G, Hendriks BS. Single-cell quantitative HER2 measurement identifies heterogeneity and distinct subgroups within traditionally defined HER2-positive patients. *Am J Pathol.* 2013;183(5):1446–1460. doi: [10.1016/j.ajpath.2013.07.015](#).
37. Moutafi M, Robbins CJ, Yaghoobi V, Fernandez AI, Martinez-Morilla S, Xirou V, Bai Y, Song Y, Gaule P, Krueger J, et al. Quantitative measurement of HER2 expression to subclassify ERBB2 unamplified breast cancer. *Lab Invest.* 2022;102(10):1101–1108. doi: [10.1038/s41374-022-00804-9](#).
38. Stavenhagen JB, Gorlatov S, Tuailon N, Rankin CT, Li H, Burke S, Huang L, Johnson S, Bonvini E, Koenig S. Fc optimization of therapeutic antibodies enhances their ability to kill tumor cells in vitro and controls tumor expansion in vivo via low-affinity activating Fcγ receptors. *Cancer Res.* 2007;67(18):8882–8890. doi: [10.1158/0008-5472.CAN-07-0696](#).
39. Li JY, Perry SR, Muniz-Medina V, Wang X, Wetzel LK, Rebelatto MC, Hinrichs MJM, Bezabeh BZ, Fleming RL, Dimasi N, et al. A biparatopic HER2-targeting antibody-drug conjugate induces tumor regression in primary models refractory to or ineligible for HER2-targeted therapy. *Cancer Cell.* 2016;29(1):117–129. doi: [10.1016/j.ccell.2015.12.008](#).

40. Larbouret C, Gaborit N, Chardès T, Coelho M, Campigna E, Bascoul-Mollevi C, Mach J-P, Azria D, Robert B, Pèlerin A. In pancreatic carcinoma, dual EGFR/HER2 targeting with cetuximab/trastuzumab is more effective than treatment with trastuzumab/erlotinib or lapatinib alone: implication of receptors' down-regulation and dimers' disruption. *Neoplasia*. 2012;14(2):121–130. doi: [10.1593/neo.111602](https://doi.org/10.1593/neo.111602).
41. Gaborit N, Larbouret C, Vallaghe J, Peyrusson F, Bascoul-Mollevi C, Crapez E, Azria D, Chardès T, Poul M-A, Mathis G, et al. Time-resolved fluorescence resonance energy transfer (TR-FRET) to analyze the disruption of EGFR/HER2 dimers: a new method to evaluate the efficiency of targeted therapy using monoclonal antibodies. *J Biol Chem*. 2011;286(13):11337–11345. doi: [10.1074/jbc.M111.223503](https://doi.org/10.1074/jbc.M111.223503).
42. Richards JO, Karki S, Lazar GA, Chen H, Dang W, Desjarlais JR. Optimization of antibody binding to FcγRIIa enhances macrophage phagocytosis of tumor cells. *Mol Cancer Ther*. 2008;7(8):2517–2527. doi: [10.1158/1535-7163.MCT-08-0201](https://doi.org/10.1158/1535-7163.MCT-08-0201).
43. Bordeau BM, Yang Y, Balthasar JP. Transient competitive inhibition bypasses the binding site barrier to improve tumor penetration of trastuzumab and enhance T-DM1 efficacy. *Cancer Res*. 2021;81(15):4145–4154. doi: [10.1158/0008-5472.CAN-20-3822](https://doi.org/10.1158/0008-5472.CAN-20-3822).
44. Cilliers C, Menezes B, Nessler I, Linderman J, Thurber GM. Improved tumor penetration and single-cell targeting of antibody–drug conjugates increases anticancer efficacy and host survival. *Cancer Res*. 2018;78(3):758–768. doi: [10.1158/0008-5472.CAN-17-1638](https://doi.org/10.1158/0008-5472.CAN-17-1638).
45. Singh AP, Guo L, Verma A, Wong GGL, Thurber GM, Shah DK. Antibody coadministration as a strategy to overcome binding-site barrier for ADCs: a quantitative investigation. *AAPS J*. 2020;22(2):28. doi: [10.1208/s12248-019-0387-x](https://doi.org/10.1208/s12248-019-0387-x).
46. Aggarwal D, Yang J, Salam MA, Sengupta S, Al-Amin MY, Mustafa S, Khan MA, Huang X, Pawar JS. Antibody-drug conjugates: the paradigm shifts in the targeted cancer therapy. *Front Immunol*. 2023;14:1203073. doi: [10.3389/fimmu.2023.1203073](https://doi.org/10.3389/fimmu.2023.1203073).
47. Baeuerle PA, Wesche H. T-cell-engaging antibodies for the treatment of solid tumors: challenges and opportunities. *Curr Opin Oncol*. 2022;34(5):552–558. doi: [10.1097/CCO.0000000000000869](https://doi.org/10.1097/CCO.0000000000000869).
48. Segal NH, Logan TF, Hodi FS, McDermott D, Melero I, Hamid O, Schmidt H, Robert C, Chiarion-Sileni V, Ascierto PA, et al. Results from an integrated safety analysis of urelumab, an agonist anti-CD137 monoclonal antibody. *Clin Cancer Res*. 2017;23(8):1929–1936. doi: [10.1158/1078-0432.CCR-16-1272](https://doi.org/10.1158/1078-0432.CCR-16-1272).
49. Geuijen C, Tacke P, Wang L-C, Klooster R, van Loo PF, Zhou J, Mondal A, Liu Y-B, Kramer A, Condamine T, et al. A human CD137×PD-L1 bispecific antibody promotes anti-tumor immunity via context-dependent T cell costimulation and checkpoint blockade. *Nat Commun*. 2021;12(1):4445. doi: [10.1038/s41467-021-24767-5](https://doi.org/10.1038/s41467-021-24767-5).
50. Shen A, Liu W, Wang H, Zeng X, Wang M, Zhang D, Zhao Q, Fang Q, Wang F, Cheng L, et al. A novel 4-1BB/HER2 bispecific antibody shows potent antitumor activities by increasing and activating tumor-infiltrating T cells. *Am J Cancer Res*. 2023;13(7):3246–3256.